Vortex Filament Evolution Subject to Pulsed/Periodic Disruption

Larry A. Young[†]
NASA Ames Research Center, Moffett Field, CA, 94035-1000

There is considerable interest within the fixed- and rotary-wing research communities as to discovering how fixed- and rotary-wing trailed tip vortices might be modified or controlled. The reasons for attempting such vortical flow control are many but success to date has been very modest. This is primarily the case because the vortical flow physics are still not adequately understood. A new analytic model describing the flow behavior resulting from pulsed or periodic disruption to line vortices is described. Such vortex filament disruption is manifested in three different forms: spatial cuts or breaks, embedded inner core negative vorticity, and/or sinusoidal varying circulation. These are three possible strategies by which vortex filament strength and geometry can perhaps be modified through passive or active control mechanisms. Finally, an additional analysis is presented that examines the feasibility of destabilizing vortical structures, thereby representing a fourth potential approach for active flow control. The presented work describes a wide array of unsteady flow phenomena that are highly pertinent to the question of active control of trailed rotary- and fixed-wing vortices.

Nomenclature

r	Radial coordinate, origin at filament axis, m
$r^\bullet$	Nondimensional radial coordinate, $r^\bullet = r/r_{c0A}$
r_{c0}	"Finite core" vortex filament core size radius (at time equal to zero), m
Re	Vortex Reynolds number, $\mathrm{Re} = \gamma/\nu$
s	Axial distance of filament breakpoint (time equal zero) from origin, m
t	Time, sec
$t^\bullet$	Nondimensional time parameter, $t^\bullet = \nu t/r_{c0A}^2$
$\mathbf{V}$	Velocity vector, cylindrical coordinates, $\mathbf{V} = \begin{bmatrix} v_r & v_\theta & v_z \end{bmatrix}$, m/sec
V_p	Finite core vortex axial flow "wave front" propagation velocity, m/sec
z	Axial (along vortex filament axis) coordinate, origin at intersection of filament segments' plane of symmetry and filament axis, m
$z^\bullet$	Nondimensional axial coordinate, $z^\bullet = z/r_{c0A}$
γ	Vortex filament initial circulation strength, m^2/sec
Γ	Vortex circulation, m^2/sec
ν	Kinematic viscosity, m^2/sec
θ	Angular coordinate, radians
$\boldsymbol{\omega}$	Vorticity vector, $\boldsymbol{\omega} = \begin{bmatrix} \omega_r & \omega_\theta & \omega_z \end{bmatrix}$, 1/sec

[†] Aerospace Engineer, Aeromechanics Branch, Flight Vehicle Research and Technology Division, Mail Stop 243-12, AIAA Associate Fellow.

I. Introduction

TRAILED tip vortex filament "modification" through various notional passive and active control schemes, to diffuse or otherwise alter the vortex, has long been the elusive goal of numerous fixed- and rotary-wing aeronautics researchers. The capability for such vortex modification is anticipated to yield a number of benefits including aerodynamic performance improvements, noise reduction, and airframe vibration improvements, e.g. Refs. 1-6. The reasons for attempting such vortical flow control are many, but success to date has been very modest. This is the case largely because the vortical flow physics are still not adequately understood.

A new analytic model describing the flow behavior resulting from the application of pulsed or periodic trains of either discrete variable circulation, spatial cuts to, and/or embedded finite regions of negative vorticity in the inner core of, vortex filaments is described. Application of such variable circulation, spatial cuts and/or injection of embedded negative vorticity are three possible strategies by which vortex filament strength and geometry can perhaps be modified through passive or active control mechanisms, Fig. 1. The analysis, having laminar origins, relies upon the artifice of the constant eddy viscosity assumption/hypothesis of Squires (Ref. 7 and more recently, e.g., Ref. 8 for similar application of this assumption to the study of rotor vortices) to extend the analysis results to turbulent vortices. Further, the analysis is founded upon the study of line vortices and not trailed vortices. As has been established since at least the work of Batchelor, Ref. 9, trailed vortices not only grow in terms of core radii with downstream distance but also have significant nonzero axial flow. Line vortices, of course, exhibit neither feature. Despite these important differences, the extended analytical work employed in this paper, based on the initial work of Refs. 10-12, has many advantages for this proposed effort, being among other things not subject to numerical diffusion as might the case for computational fluid dynamics models, whereby the spatiotemporal evolution of vortex filaments can be studied.

A wide array of unsteady flow phenomena is captured by this analysis. It was originally derived to study axisymmetric vortex reconnection, and/or breakdown, subsequent to severe perpendicular/orthogonal body/blade-vortex interactions. The nature of this original problem necessitated developing the inherent analysis capability to predict the influence of discrete changes in the vortex filament's vorticity distributions. This same capability provides great utility for the current problem. The influence on the vortex spatiotemporal evolution, as a consequence of these vorticity distribution changes, are highly pertinent to the question of active vortical flow control of trailed vortices.

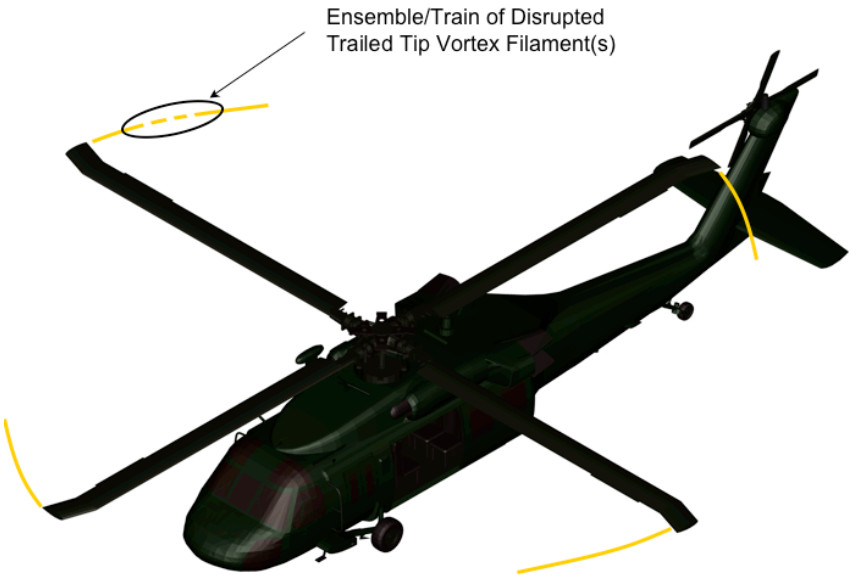

Fig. 1 -- Modifying or Disrupting Trailed Tip Vortices (for Rotorcraft)

II. Past Investigations/Approaches to Vortical Flow Active Control

For rotorcraft, for reducing blade-vortex interaction (BVI), there are two fundamental stratagems to pursue: first, increase the miss distance between the trailed vortex and the following rotor blade(s), and, second, somehow dissipate, or otherwise reduce the strength of the vortex at the location of the interaction. This work primarily discusses the implications of the later approach: modifying or disrupting vortices so as to reduce their potential for adversely interacting with, such as impulsively loading, rotor blades and/or other surfaces. For BVI phenomena not entailing very close passage of the vortex near a rotor blade, vortex modification will only have a secondary influence, as the vortex-induced velocities will adhere to a $1/h$ functionality, where h is the miss-distance, for all but the closest miss-distances to the vortex spanwise axis. For these particular types of blade-vortex interactions increasing the blade miss-distance, by attempting to globally tailor the near-field rotor wake, is likely the only effective means of moderating overall interactions. It is only those most severe of blade-vortex interactions wherein the blade comes in very close proximity to, or even physically intersects/collides with, the trailed vortex does it seem feasible that modifying the vortical structure (near or within the core) of the vortex might result in alleviation/moderation of the BVI event.

As noted earlier, representative work in Refs. 1-6 detail numerous attempts to modify (actively and passively) rotary- and fixed-wing trailed tip vortices. The anticipated benefits for modifying the vortical flow characteristics for these trailed vortices ranges from blade-vortex-interaction noise, vibration, and load reduction for rotorcraft to wake hazard alleviation for fixed-wing aircraft. Table 1 summarizes, and Fig. 2a-g depicts, some of the various flow control approaches studied to date and their possible underlying vortical flow mechanisms. In many cases, the vortical flow structure of the rotor and wing trailed vortices have been successfully modified through several of these approaches, as demonstrated both analytically and experimentally. However, in most cases, such vortical flow control has been found to be either unreliable, inconsistent, or, alternatively, requires too large of a performance penalty to be successfully implemented on an actual flight vehicle. Additionally, previous work has suffered from a lack of robust metrics and criteria for defining/assessing success in vortex modification or disruption. Typically, researchers in the past have focused on a general qualitative assessment of the ability to engender trailing vortex core growth and/or reductions in maximum tangential velocity. Only rarely has the question of the "extent" and "persistence" of such vortex modifications been considered. The current work seeks to define more rigorous metrics for vortex modification and disruption, which inherently take into account questions of extensiveness and persistence of changes made by vortical flow control.

Table 1 – Vortical Flow Control Strategies Noted in the Literature and their Possible Mechanisms that could be simulated by Current Analysis

Flow Control Approach	Spatial "Cut" or "Break"	Sinusoidal Varying Circulation	Embedded Vorticity	Excitation or Destabilization
Spanwise Blowing	X		X	X
"Synthetic-Jets"			X	X
"Spoilers"	X		X	X
Vortex Generators			X	X
"Sub-wings"			X	X
Blade Tip Modification	X		X	X
Active Elevons		X		X
Individual Blade Control		X		X
Active, or "Free," Tips	X	X		X

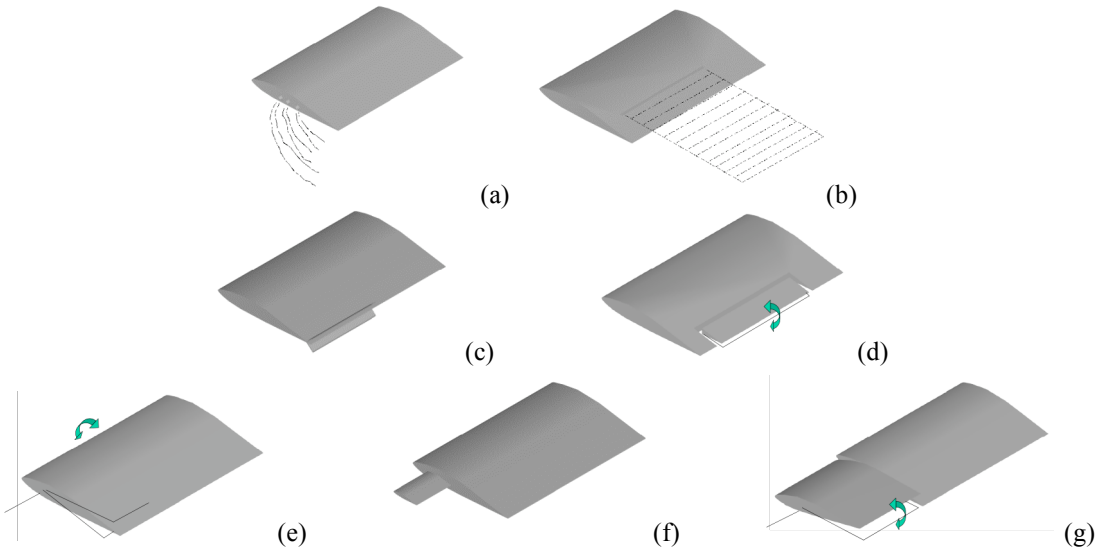

Fig. 2 – Different Actuator Approaches to Rotor Vortical Flow Control: (a) Spanwise Blowing, (b) "Synthetic-Jet" or "Zero-Mass" Actuator, (c) Spoilers, (d) Active Elevons, (e) IBC, (f) Stub-wings, and (g) Active/Free Tips

In all of the above cases, there appears to be two fundamental, though not necessarily mutually exclusive, vortical flow control approaches being proposed by the research community for near-field (or, rather, early wake age in the case of rotor tip vortices) vortex modification/disruption. The first fundamental approach is where the "bulk properties" of the vortex are modified. In other words, the vortex strength and geometry is somehow directly modified during early roll-up or trailing from the rotor or wing. The second fundamental approach seeks to somehow destabilize or otherwise excite the trailed vortices to have them transition from one (basic) flow state to another, notionally more benign, flow state through either flow instability (i.e. vortex breakdown) or laminar-to-turbulent transition mechanisms. Instigating vortex destabilization is particularly appealing to investigators, as it seems to almost promise a "free lunch" approach to vortex modification. But rarely questioned is the issue of destabilization to *what*? What alternate flow state are these vortices being nudged towards? Most full-scale rotor trailed tip vortices are undoubtedly already turbulent throughout most of their core structure. Therefore, artificially attempting to effect vortex laminar-to-turbulent flow transition would seem to be a pointless exercise. The alternate, in terms of notionally achievable flow states, is vortex breakdown, whereby large changes in vortex core size and strength, with corresponding axial flow stagnation points under a variety of circumstances can be suddenly manifested. However, vortex breakdown is not universally considered a flow instability, per se. For example, Refs. 10-12 demonstrated that axisymmetric vortex breakdown can result from the same type of bulk property modifications as will be studied in this paper, without resorting to any form of generally recognized instability mechanism. Irregardless, examples of both the "bulk property" and "destabilization" approaches will be studied in this paper, though the primary focus will be on the direct modification of vortex bulk properties through various general notional techniques of disrupting the vortices.

III. Summary of Analytical Treatment

References 10-12, examined the unsteady flow characteristics of "cut" vortex filaments with one or two breakpoints (Fig. 3). This earlier work would suggest that vortex reconnection is re-established fairly quickly in terms of nondimensional time scales with only modest localized disruption of the vortex vorticity and circulation distributions. This is an indirect testament to the difficulty of modifying vortex strength and geometry -- which, in part, is explanatory of the complementary empirical difficulties in

accomplishing the self-same goal. Nonetheless, the previous analytical work has provided some tantalizing clues as to the possibility of employing pulsed/periodic vortex disruptions (as implemented as vortex filament "cutting" with multiple (more than two) breakpoints or, alternatively, the injection of negative vorticity into the vortex inner core) yielding the desired vortex modifications. Validation of this hypothesis, and consideration of the necessary and sufficient conditions for such radical vortex modifications is the subject of the current work.

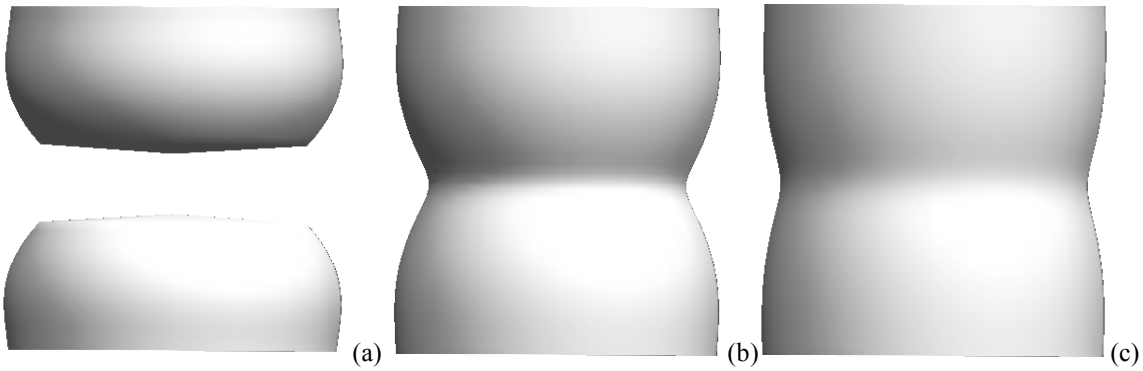

Fig. 3 -- Vortex Core Size Spanwise Variation During Vortex Filament Reconnection ("parabolic" core with no axial flow prior to "cutting" and a single filament cut ((a) $t^{\bullet} = 0.01$, (b) $t^{\bullet} = 0.05$, and (c))

A class of unsteady laminar flow problems called "moving boundary" problems has been exhaustively studied in the literature. By assuming that $v_r = v_z = 0$, the Helmholtz vorticity equation, for axial vorticity, can be reduced to the well-known unsteady heat conduction equation (Ref. 13). The Lamb-Oseen vortex solution (Ref. 14) is one member of this class of unsteady laminar flow problems. It is proposed that a class of solution be defined by assuming that the radial velocity component, v_r, is not merely equal to zero but instead is proportional to the tangential velocity gradient with respect to the z-axis (Eq. 1). (Note that if the tangential velocity gradient is zero, such as in the case of the Lamb-Oseen vortex, then the "moving boundary" class of problems is recaptured.)

$$v_r \propto \frac{\partial v_\theta}{\partial z} \tag{1}$$

Or

$$v_r = \ell \frac{\partial v_\theta}{\partial z} \tag{2}$$

The length scale factor, ℓ, is a constant -- at least within a given discrete spatial region(s) -- that transforms the proportional relationship of Eq. 1 to the equivalence relationship of Eq. 2. (The constant ℓ has the unit of length - hence it being called a "length scale factor.") This is discussed in detail in Refs. 10-12.

Meanwhile, a second proportional relationship, based on flow continuity, can be defined for the axial velocity.

$$v_z \propto -\left(\frac{\partial v_\theta}{\partial r} + \frac{v_\theta}{r} \right) \tag{3}$$

Or

$$v_z = -\ell\left(\frac{\partial v_\theta}{\partial r} + \frac{v_\theta}{r}\right) \tag{4}$$

This in turn dictates that the vorticity can be related to the velocity components, via the divergence equations for vorticity.

$$v_z = -\ell\omega_z$$

$$v_r = -\ell\omega_r \tag{5a-b}$$

Applying a length-scale factor causes the convective acceleration terms to cancel out the vortex stretching terms, thereby achieving the objective of reducing the Helmholtz equation to the unsteady heat conduction equation, e.g. (Eq. 6) for the axial vorticity.

$$\frac{D\boldsymbol{\omega}}{Dt} = (\boldsymbol{\omega}\cdot\nabla)\mathbf{V} + \nu\nabla^2\boldsymbol{\omega}$$

$$\downarrow$$

$$\frac{\partial\omega_z}{\partial t} = \nu\left\{\frac{\partial^2\omega_z}{\partial r^2} + \frac{1}{r}\frac{\partial\omega_z}{\partial r} + \frac{\partial^2\omega_z}{\partial z^2}\right\} \tag{6}$$

It is important to note that the length-scale factor methodology yields solutions that are only approximate in nature. Though the Helmholtz equation for axial vorticity is exactly satisfied, for the cases where $\omega_r \neq 0$ and $\omega_\theta \neq 0$, i.e. non-columnar flow, the corresponding equations for the radial and azimuthal vorticity are satisfied only approximately. More details as to the underlying general nature of the approximations and their consequences are given in Refs. 10 and 12.

Four different approaches to pulsed or periodic disruption of vortex filament will be studied using the length scale factor analysis methodology: vortex disruption via "cutting," disruption through periodic injection of flow with negative vorticity into the inner core of the vortex, sinusoidal varying vortex circulation, and vortex destabilization. (The later analysis will be summarized in the Appendix.) This work is an extension of the "multiple breakpoint" and "finite-segment" vortex filament analysis presented in Ref. 12. Some representative results are presented in Figs. 4-6 showing the axial distribution (along the vortex filament axis) of enstrophy and vortex core size subject various pulsed/periodic disruptions to the line vortices. It should be noted that among the parametric influences examined in this paper are the magnitude, frequency, and sequencing of such pulsed/periodic disruptions. Therefore, as can be seen in Fig. 4, the vortex filament "ideal cuts" are not uniform in spacing between breakpoints. Correspondingly, in Fig. 5, the embedded regions of negative vorticity in the vortex inner core are not uniform in spanwise expanse. Figure 6 shows illustrative examples of enstrophy and core size distributions due to sinusoidal variation of the vortex circulation along its span. It is anticipated that such "tailoring" of pulsed/periodic trains of vortical flow disruption will be a key factor in maximizing the effectiveness of vortex modification. Finally, it is assumed that the localized ensemble of vortex disruptions analyzed is of small enough span, in terms of range of nondimensional axial coordinate, $z^\bullet$, that any axial variation of trailed vortex core size and strength can be ignored for the purposes of this study. The analysis is limited to assuming initially zero axial flow along the vortex, which is not, in general, representative of trailed tip vortices.

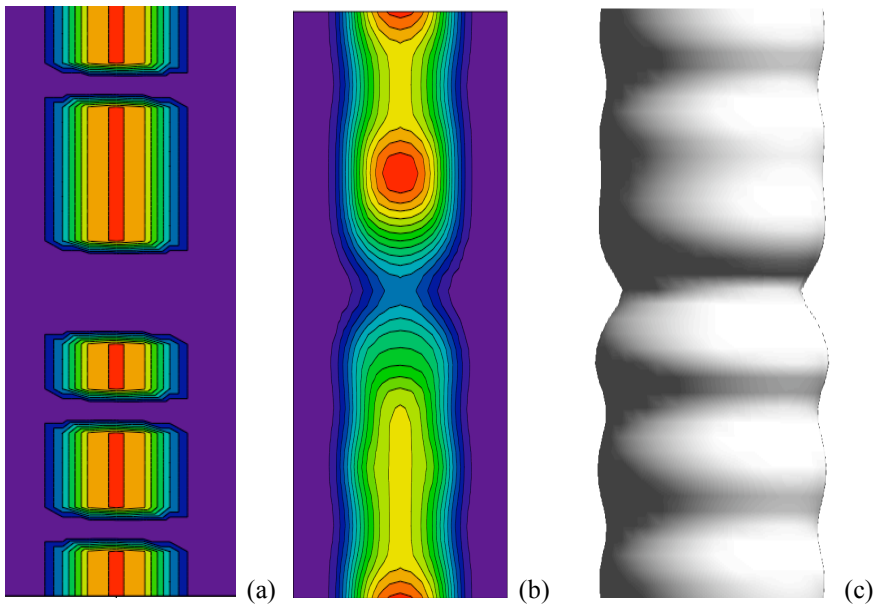

Fig. 4 -- Disruption due of a Vortex Filament With Ideal "Cuts" with Multiple Breakpoints: (a) axial vorticity ($t^{\bullet} = 0$), (b) axial vorticity ($t^{\bullet} = 0.03$), and (c) vortex core size axial distributions ($t^{\bullet} = 0.03$)

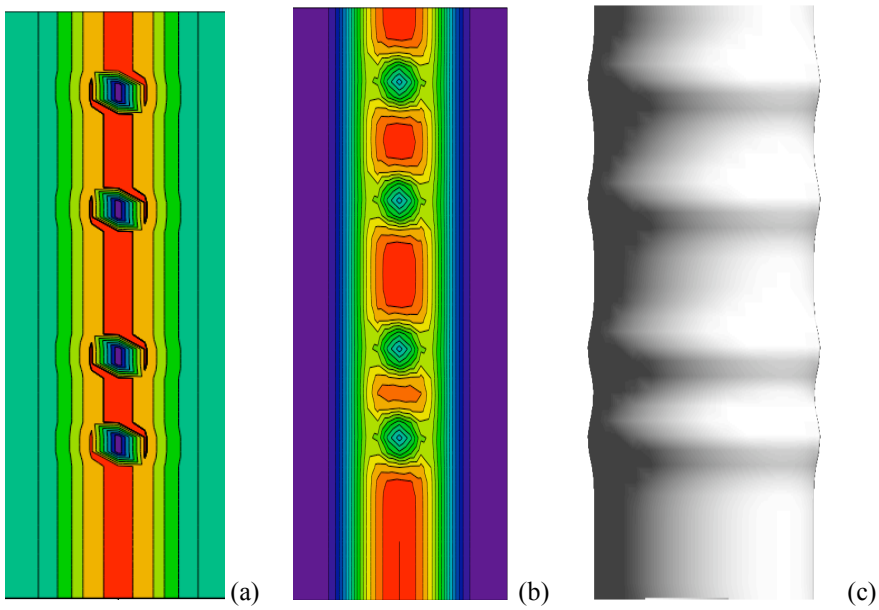

Fig. 5 -- Disruption due to Multiple Embedded Regions of Negative Vorticity being Injected/Inserted into the Inner Core of the Vortex Filament: (a) axial vorticity ($t^{\bullet} = 0$), (b) axial vorticity ($t^{\bullet} = 0.03$), and (b) vortex core size axial distributions ($t^{\bullet} = 0.03$)

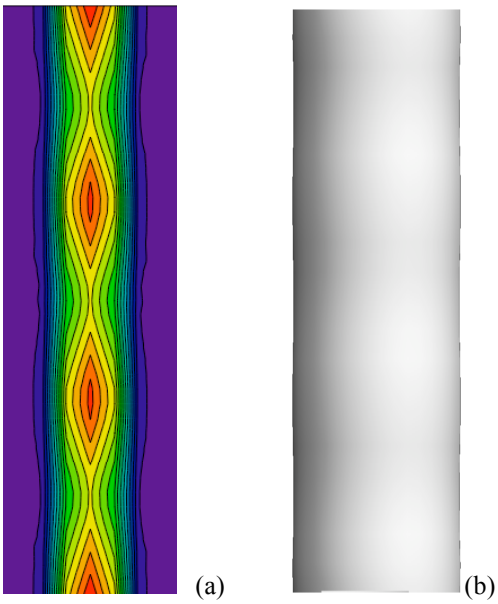

Fig. 6 -- Periodically Varying Circulation ($M = 3$, or $\lambda^{\bullet} = 1.67$, $\Delta\Gamma \approx 0.2$, and $t^{\bullet} = 0.01$): (a) Enstrophy and (b) Vortex Core Size

Any modification of the vortical flow, by any of the three approaches identified in this paper as to disrupting the vortex filament, must be considered "transitory." Inevitably, vortex filaments will reconnect as long as the filament breakpoints remain in close proximity to each and are not displaced by other self-induction or other wake influences. Modified velocity profiles will tend to evolve over time to the same asymptotic profiles. Even vortex breakdown bubbles will tend to dissipate/collapse (unless sustained in some quasi-steady manner) as a consequence of viscous diffusion. But, with appropriate control over magnitude and timing/duration, even transitory changes to vortex filament characteristics could potentially have a beneficial influence over a number of important aerodynamic and aeromechanic challenges such as blade-vortex-interaction noise and vibration reduction for rotorcraft.

One of the key problems previous researchers have had in evaluating their vortical flow active control devices is the use of inconsistent and/or qualitative metrics defining "success" in modifying the vortical flow. Typically, "success" has been defined in terms of increased vortex core size in conjunction with decreased peak swirl/tangential velocity. These are perhaps necessary, but insufficient, criteria for successful modification/disruption (a.k.a "diffusion") of rotor vortices. For example, such criteria, in part or as a whole, do not account for nonzero vortex velocity components in addition to the swirl velocity. Further, such criteria do not consider the aggregate effect of vortex disruption – i.e. is the reduced swirl and/or increased core size a localized effect, with possible aggravated vortex characteristics removed from the localized improvement, or is the modification persistent and expansive in nature. As will be discussed in the next section, two metrics will be defined/derived that embody the notion that "success" for rotor tip vortex modification or disruption (as related to bulk properties) can be defined in terms of reducing an aggregate measure (spatiotemporally integrated so as to yield a non-localized assessment) of the vortex total kinetic energy (and, therefore, the induced dynamic pressure). Tying such metrics to the vortex total kinetic energy and dynamic pressure should yield physically meaningful insights into BVI reduction for close-passage interactions between trailed vortex filaments and following blades (where the induced velocity from the vortex can analogously be thought of like a transient response to a localized flow field disturbance). Such a dynamic pressure analogy would be expected to breakdown if orthogonal blade/vortex collisions or "cutting" occurs. In this latter case, the vortex vortical structure would be radically changed as a consequence of the orthogonal BVI event and the pre-collision vortex characteristics (modified or otherwise) may or may not be indicative of the severity of such strong interactions.

IV. Performance Metrics for Vortex Modification/Disruption

It is essential to define one or more performance metrics to assess the efficacy of various different strategies for vortex modification or disruption. Two such metrics, η_V and β_V, will be defined for evaluating the performance of the vortical flow control strategies studied in this paper. The parameter η_V can be thought of as vortical flow control effectiveness and the parameter β_V can be thought of a flow control efficiency metric. Both parameters are defined in terms of the total kinetic energy, and, correspondingly, of the vortex-induced dynamic pressure, of the basic flow. The modified and baseline vortices is spatiotemporally integrated across the prescribed limits: $0^+ \le r \le \infty^-$, $0 \le t \le T$, and $-L/2 \le z \le L/2$. Two of these limits reflect the design target spatial *extent* of the vortex modification in terms of axial span of the vortex initially modified, L, as well as the design target *persistence* of the vortex modification, T (in terms of kinetic energy and dynamic pressure). The greater the targeted extent and persistence of the vortex modification/disruption the greater the initial kinetic energy investment required. In the case of rotary-wing applications there is likely a strong coupling between the T and L design targets; in this case $L \approx O(c) \approx O(\pi R\sigma/N)$, or the extent of modification should be on the order of the rotor blade chord length, and, further, $T \ge 2\pi/N\Omega$, the vortex modification/disruption has to persist to at least the first (following) blade passage. Refer to Fig. 7. Left unanswered in this paper, though, is the question of flow control actuator "mechanical" efficiency. Such mechanical efficiency is highly dependent upon the actuator design and its system integration.

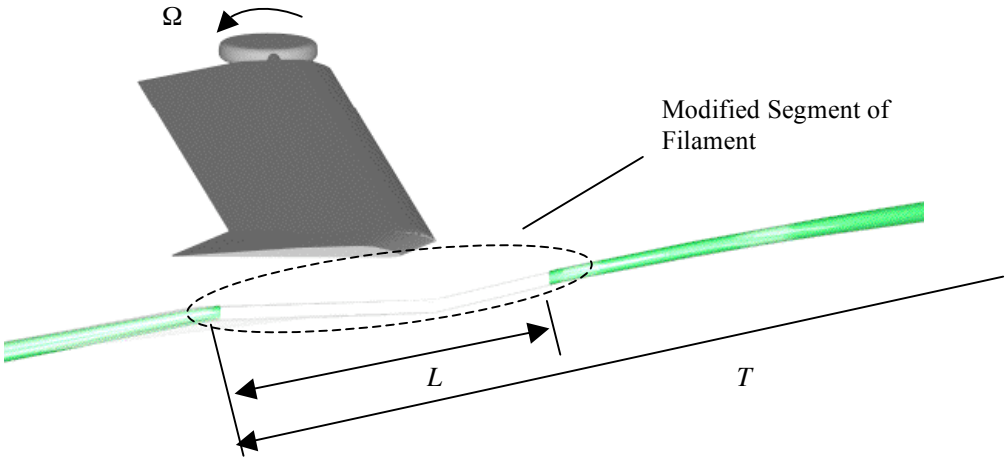

Fig. 7 – Extent, L, and Persistence, T, of Vortex Filament Modifications for Rotors

The baseline vortex, unless otherwise specified, has a parabolic initial vorticity distribution ($\chi_A = 0$ as defined in Ref. 12). The first metric, vortex modification effectiveness, is defined by the expression

$$\eta_V \equiv \eta_{BV} / \eta_{MV}$$

Where

$$\eta_{BV} = \int_{0^+}^{T} \int_{-L/2}^{L/2} \int_{0^+}^{\infty^-} \xi r dr dz dt \Big|_{Baseline\ Vortex}$$

$$\eta_{MV} = \int_{0^+}^{T} \int_{-L/2}^{L/2} \int_{0^+}^{\infty^-} \zeta r dr dz dt \Bigg|_{Modified\ Vortex}$$

And

$$\varphi_V = \varphi_{BV} / \varphi_{MV}$$

Where

$$\varphi_{BV} = \int_{-L/2}^{L/2} \int_{0^+}^{\infty^-} \zeta r dr dz \Bigg|_{\substack{Baseline\ Vortex \\ t=0^+}}$$

$$\varphi_{MV} = \int_{-L/2}^{L/2} \int_{0^+}^{\infty^-} \zeta r dr dz \Bigg|_{\substack{Modified\ Vortex \\ t=0^+}}$$

Further, given the above,

$$\beta_V \equiv \frac{\eta_V - 1}{\varphi_V - 1}$$

$$\zeta \equiv v_\theta^2 + v_r^2 + v_z^2$$

(7a-h)

Note that the parameter φ_{BV} has a simple analytical solution. The higher the relative values of η_V and β_V the better the particular vortical flow control strategy (and the parametric combination specifying that flow control). There are no intrinsic upper or lower limits to η_V and β_V as currently formulated. The majority of the discussion that follows will be centered on the estimated relative values of η_V and β_V through either vortex filament cutting, injection of negative vorticity into the vortex core, or periodic manipulation of the vortex circulation and/or core size. The vortical flow control effectiveness and efficiency metrics are estimated via numerical integration and are not analytically solved for.

V. Discussion of Results

Four different approaches to pulsed or periodic disruption of vortex filaments, and the resulting vortex modification, will now be studied, in part, using the efficiency and effectiveness metrics presented in the last section.

To put things in perspective, the time scale for these results is rather large when considering the possible influence of these vortex modification/disruption strategies for near-field rotary-wing applications such a blade-vortex interaction alleviation/moderation. Given the general nature of the analysis, and the nonlinear functions inherent in it, it is very difficult to make flow predictions at very small nonzero values of time. From a practical matter, for the work performed herein, this cut-off is approximately around $t^\bullet \approx 0.007$, quite a small value in terms of nondimensional time. In terms of actual units of time, though, this is on the order of tens of minutes for laminar flow and typically less than a minute for fully turbulent flow, where the effective turbulent viscosity can be an order of magnitude greater than the kinematic viscosity. Looked at in another way, blade-vortex-interactions typically occur within 60 to 200 degrees of wake age, depending on whether the BVI event occurs on the advancing or retreating side of the rotor. Therefore, such BVI events occur within fractions of seconds of release from the blade they're trailed from. There is, therefore,

potentially a mismatch between the time scales in the analysis versus that for rotor BVI. The analysis suffers from numerical stability issues at very small nonzero time scales ($t^{\bullet} < 0.007$). This is somewhat disadvantageous, but from a practical sense does not have that much impact as, in general, an alternate asymptotic formula has been derived for the initial condition case, $t^{\bullet} = 0$.

A. Vortex Modification via "Cutting"

The work of Ref. 12 only considered the case of ideal "cuts" to vortex filaments, where the circulation in the intermediate region between breakpoints is zero. This analysis has been extended to consider the cases of non-ideal "cuts," or otherwise referred to as "breaks," wherein the circulation in the intermediate region between "breakpoints" is not identically equal to zero but rather some nonzero fraction of the nominal vortex filament far-field circulation strength. Such a representation of vortex filament "breaks" is likely more physically realistic than the case of ideal "cuts." Figure 8a-d presents a representative subset of single filament breaks for a number of different fractional circulation strengths between the vortex breakpoints.

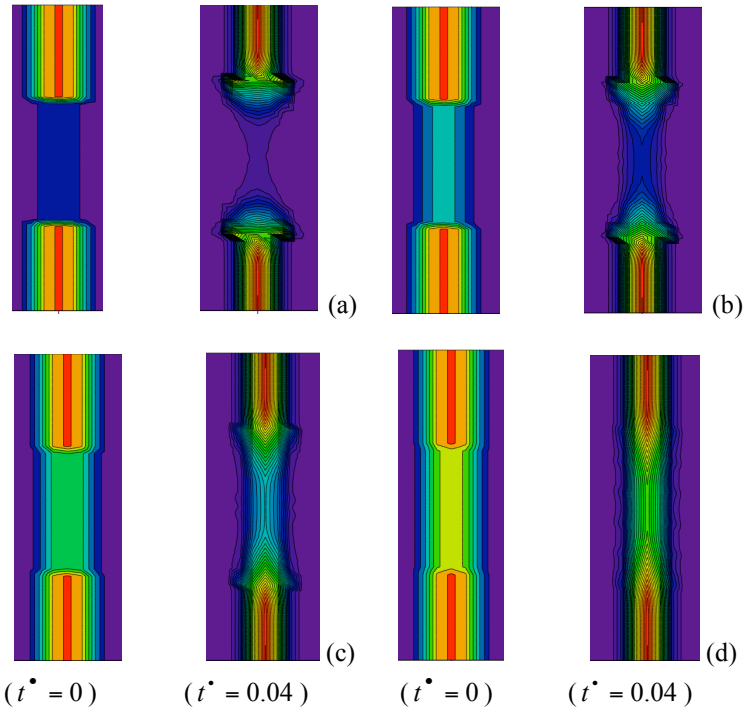

Fig. 8 – Enstrophy Contour Time Trends (Non-ideal Cuts, a.k.a. "Breaks," $s/r_{c0} = 2$): (a) residual circulation in the intermediate region, $\gamma/\gamma_{\infty} = 0.2$, (b) $\gamma/\gamma_{\infty} = 0.4$, (c) $\gamma/\gamma_{\infty} = 0.6$, (d) $\gamma/\gamma_{\infty} = 0.8$

Figure 9 illustrates the time evolution of the vortex filament kinetic energy as a function of time for the case of "cut" vortex filaments at fixed span between breakpoints, $s/r_{c0} = 2$. As anticipated as time increases the kinetic energy decreases as a consequence of vortex diffusion. The kinetic energy, as a whole, is directly proportional to the sum total span relative to the ensemble length, L, of the individual intermediate regions between filament breakpoints.

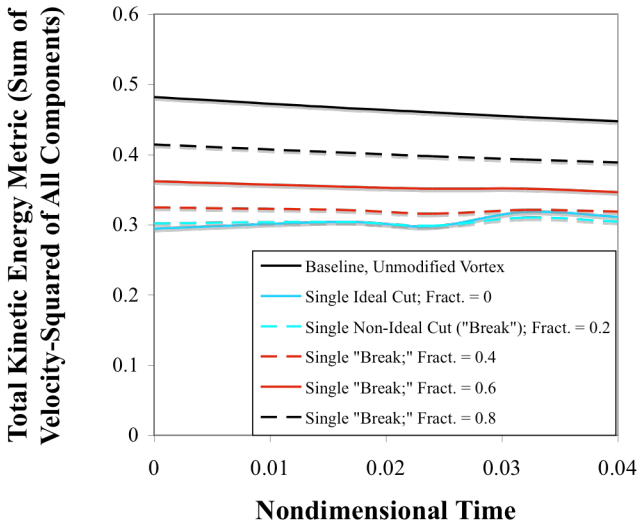

Fig. 9 – Trend of Total Kinetic Energy Metric ($\left(v_\theta^\bullet\right)^2+\left(v_r^\bullet\right)^2+\left(v_z^\bullet\right)^2$) as a Function of Nondimensional Time

Individual velocity component kinetic energy metrics are presented in Fig. 10a-c for a single non-ideal "break" (at fixed span between breakpoints, $s/r_{c0} = 2$) where the fraction of the circulation strength within the intermediate region between breakpoints is held (spanwise) constant at a range of values of γ/γ_∞

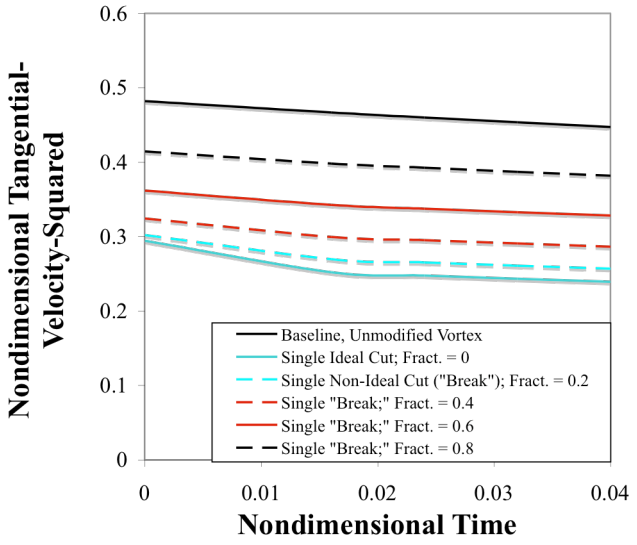

(a)

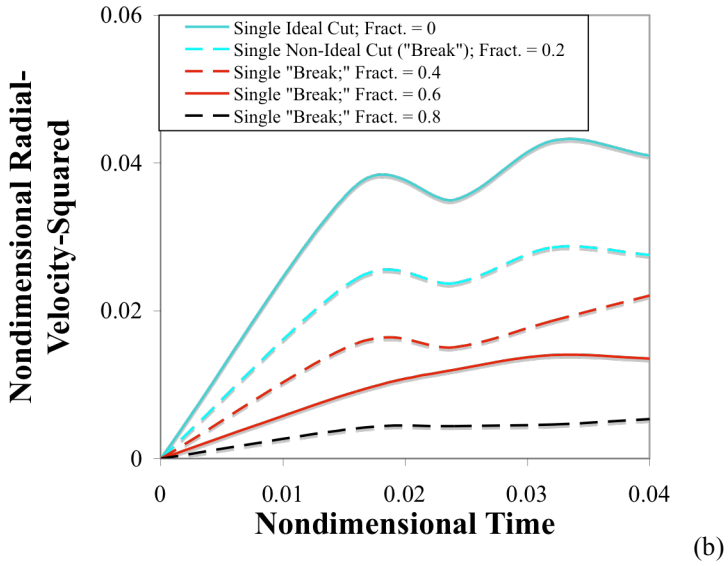

(b)

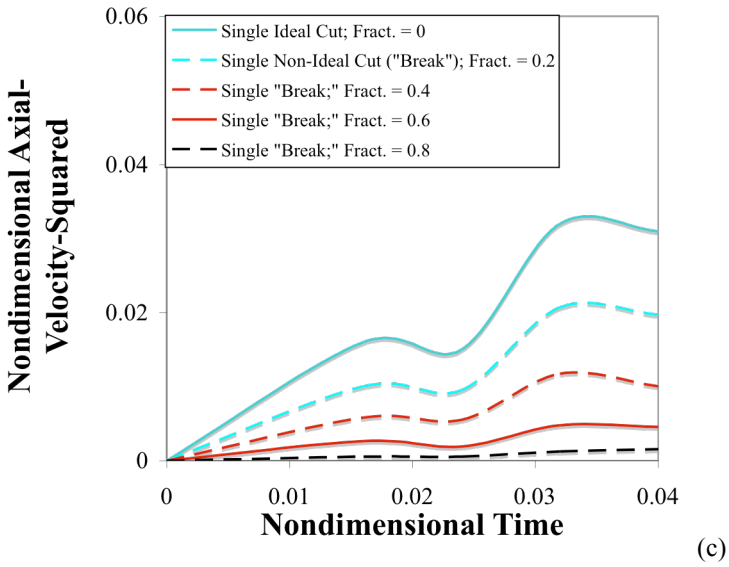

(c)

Fig. 10 – Individual Velocity Component Kinetic Energy Metrics with Respect to Nondimensional Time (Single Non-ideal "Break"): (a) Tangential ($\left(v_\theta^\bullet\right)^2$), (b) Radial ($\left(v_r^\bullet\right)^2$), (c) Axial ($\left(v_z^\bullet\right)^2$)

Given this new capability of analyzing vortex filaments with physically more relevant "breaks," the efficacy of such filament "breaking" is examined as to a possible means for modifying/disrupting a vortex in a beneficial manner so as to attenuate its dynamic pressure distribution. Figure 11 presents the corresponding results of the vortex modification/disruption effectiveness and efficiency of single vortex filament "breaks" for a range of (constant) fractional circulation strengths between breakpoints.

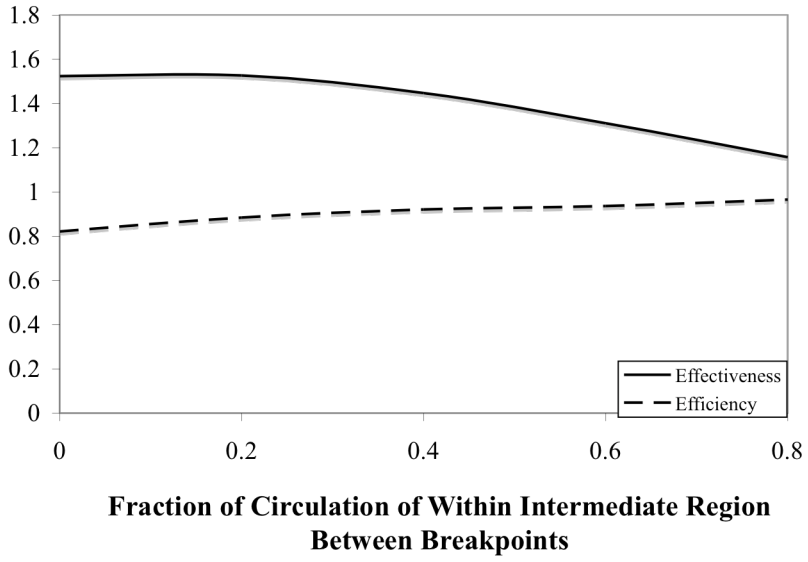

Fig. 11 – Efficiency and Effectiveness Trends (for Single Non-ideal Cuts, a.k.a. "Breaks")

B. Vortex Modification via Periodic Injection of Negative Vorticity

An alternate approach to vortex modification is through vortex disruption via periodic injection/application of negative vorticity into the inner core of the vortex. Such injection/embedding of incremental vorticity (in general either positive or negative) can be implemented such that either the circulation is reduced in a localized sense or is, alternatively, preserved. Figure 12 shows the enstrophy distribution for a vortex filament with a single embedded region of negative vorticity (that embedded vorticity being described by the two parameters χ_A and η_A) whereby the circulation is reduced in a localized sense.

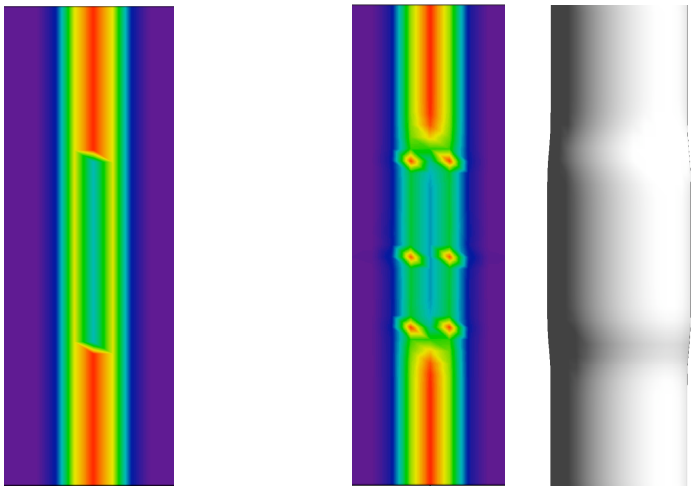

$(t^{\bullet} = 0)$ $(t^{\bullet} = 0.04)$

Fig. 12 – Representative Enstrophy Distributions as a Function of Time for the Injection of a Single Embedded Region of Negative Vorticity (Reduced Circulation; $\chi_A = -0.1$ and $\eta_A = 0.25$)

Figure 13 presents predicted results for the injection/insertion of a single region of embedded negative axial vorticity ($\chi_A = -0.1$ and $\eta_A = 0.25$) of varying nondimensional span ($1 \le s/r_{c0} \le 4$). As a consequence of the embedded inner core negative vorticity a localized reduction of vortex circulation results. This in turn reduces the ensemble average of the vortex total kinetic energy and thereby resulting in an increasing vortex modification effectiveness metric with increasing span (and, therefore, total quantity) of the embedded region of negative vorticity.

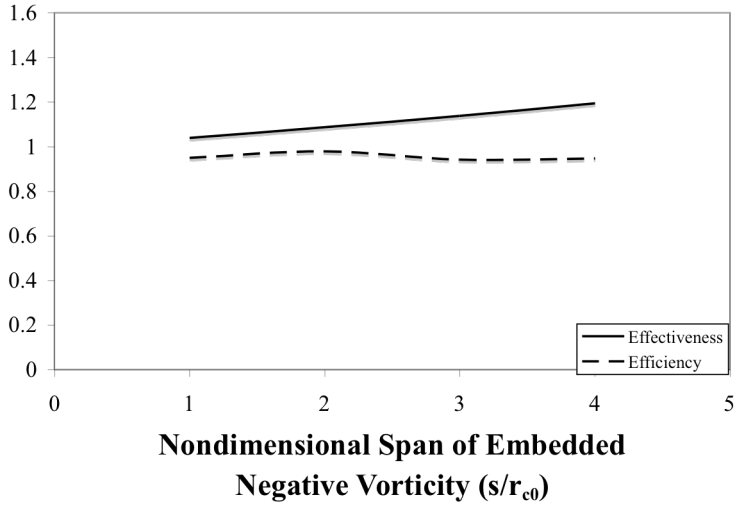

Fig. 13 – Influence of Embedded Negative Vorticity in the Inner Core (with no Vortex Filament Cuts/Breaks) as a Function of the Span of the Embedded Region

The individual influence of vortex filament cutting and injection/insertion of negative vorticity into the vortex core appears to have only modest effectiveness as means of modifying/disrupting vortices. But what of combined effects simultaneously applying the two vortical flow control approaches. Earlier studies on vortex reconnection and breakdown phenomena, Refs. 10-12, would suggest that if the physical mechanism of effecting vortex filament cutting/breaking also engenders the generation/transfer of negative vorticity at or into the vortex inner core then vortex breakdown occurs during the course of the vortex reconnection process. Instigation of such a vortex breakdown would likely radically reduce the total kinetic energy. The fact that such a vortex breakdown stems from a modification of the bulk properties of the vortex, rather than relying on some notional instability mechanism, provides hope that a reliable actuator mechanism might be devised.

Figure 14 illustrates the effect of the combined vortex filament cutting (single ideal cut of $s/r_{c0} = 2$) with insertion of negative vorticity (a single region of $span/r_{c0} = 2$, $\chi_A = -0.3$, and $\eta_A = 0.375$) on the vortex core size and also shows the formation of a vortex breakdown bubble. The localized increase vortex core size and the formation of a breakdown bubble have been previously predicted in Ref. 12.

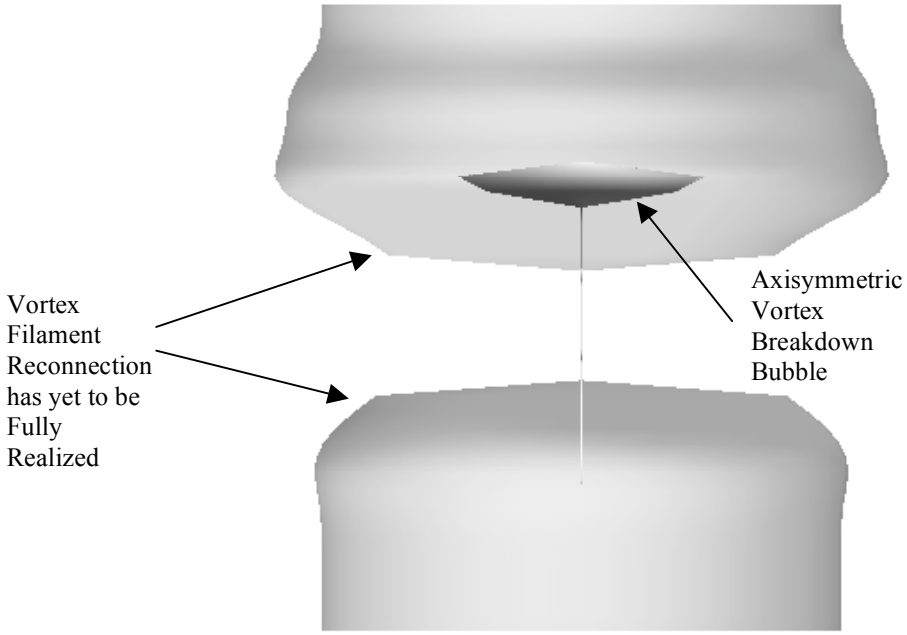

Fig. 14 – Vortex Filament Cutting/Breaking "Seeded" with Negative Vorticity

Figure 15 presents predicted vortex modification effectiveness and efficiency metric results, for a single ideal cut ($s/r_{c0} = 2$) in conjunction with a single embedded region of negative vorticity (the span of which ranges from $0.5 \le span/r_{c0} \le 2$ and, further, $\chi_A = -0.3$, and $\eta_A = 0.375$). (Note that the ensemble average is conducted over the temporal range of $0.01 \le t^{\bullet} \le 0.05$ rather than at $0 \le t^{\bullet} \le 0.04$ as done previously.) It is anticipated that the observed increase in core size and corresponding reduction in localized kinetic energy, Figs. 14 and 15, will be moderated somewhat with the implementation of non-ideal cuts, or rather filament breaks, but that, in general, the relative trends observed should still be applicable.

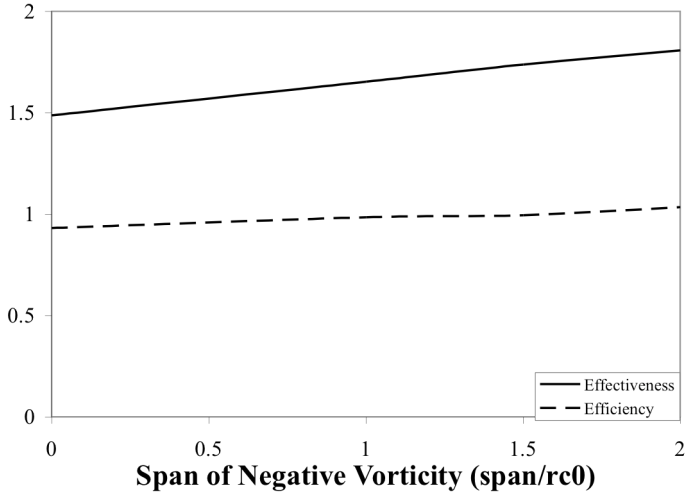

Fig. 15 – Vortex Modification Effectiveness and Efficiency as a Result of Combinations of Filament Cutting/Breaking and Application of Negative Vorticity

Therefore, it would appear that given sufficient span/magnitude of embedded negative vorticity, in conjunction with vortex filament cutting or breaking, that an additional augmentation of vortex modification can occur. However, below a threshold level of negative vorticity (in terms of span), the effectiveness metric is lower than filament cutting/breaking applied by itself. This augmentation in vortex modification effectiveness is primarily a result of inducing a significant region of vortex breakdown in the vortex filament, through the combined application of these two bulk property changes (as distinguished from vortex "destabilization"). This notional approach to vortical flow control was found to be the most effective means of vortex modification or disruption studied in this paper.

C. Vortex Modification via Periodically Varying Circulation

Sinusoidal variations of vortex circulation along the filament axis can only be approximately modeled, or perhaps more correctly "simulated," by the analysis employed in this paper. The approximations entailed are fourfold. First, though the circulation is periodic, the spanwise distribution is only an approximate sinusoid. Second, the circulation is only varied within the spanwise limits within which the ensemble average is performed to define the effectiveness and efficiency metrics. And, third, there can be "edge effects" depending upon how the circulation strength is specified at the spanwise limits employed in the ensemble average. Fourth, and final, at the small, but nonzero, time value for which the temporal averaging is initiated, the radial and axial velocity components are subtracted out as "offset tares" so as to better simulate the anticipated physical flow entailed in the periodic variation of vortex circulation. Figure 16 presents some representative spanwise vortex circulation distributions as a function of the distributions nondimensional "wavelength," $\lambda^{\bullet}$. This nondimensional wavelength can be defined in terms of both the nominal sinusoid's cycle count, M, and the span of the ensemble region, L, i.e. specifically, $\lambda^{\bullet} \equiv L/2Mr_{c0}$. In Fig. 16, the circulation is varied peak-to-peak by 20%, i.e. $\Delta\Gamma \approx 0.2$. Additionally, though the circulation varies approximately in a sinusoidal manner for $|z| < L/2$, for $|z| \geq L/2$ the circulation is held constant at $\Gamma = 1 + \Delta\Gamma/2$. Finally, by way of a reminder, for all work presented in this paper, a single ensemble limit applies. i.e. $L = 10r_{c0}$. For a typical helicopter trailed tip vortex where the near-wake vortex core size radius ranges from 5 to 10% of the blade chord, L would, therefore, represent a span of a trailed tip vortex filament of approximately one-half to one chord length. This in turn translates to an azimuth increment of the rotating blade of 2 to 4 degrees for the blade (at near the tip) to traverse a distance of L.

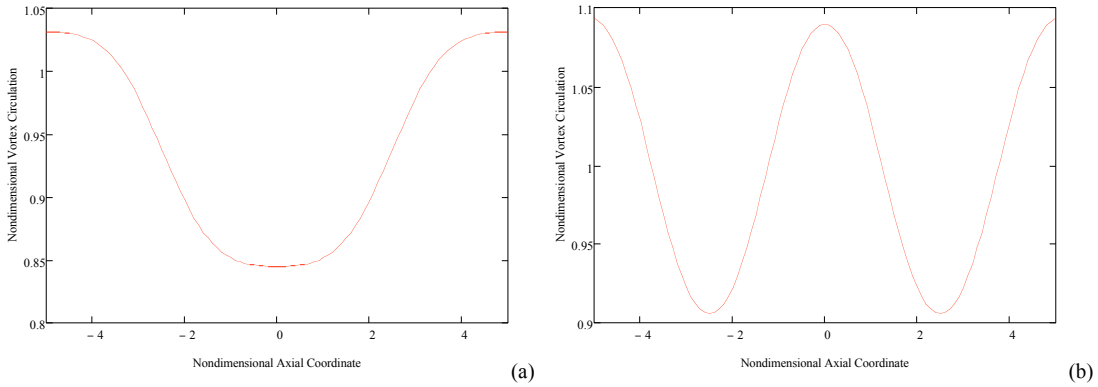

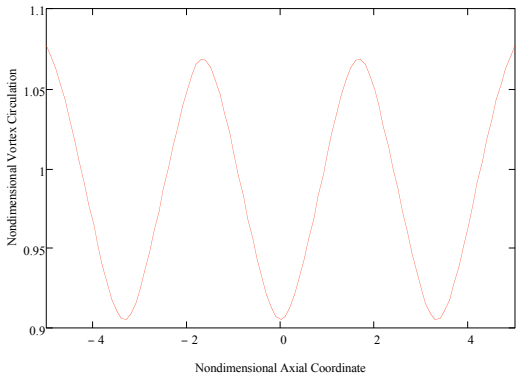

(c)

Fig. 16 – Spanwise Circulation Distributions as a Function of Periodic "Wavelength ($\Delta\Gamma \approx 0.2$):" (a) $\lambda^{\bullet} = 5$ (M=1), (b) $\lambda^{\bullet} = 2.5$ (M=2), and (c) $\lambda^{\bullet} = 1.67$ (M=3)

Figure 17 presents representative results for the influence of periodically varying the vortex circulation (while insuring the "mean" spanwise circulation is kept constant) on the vortex modification/disruption effectiveness and efficiency parameters. The magnitude of the circulation is modest, $\Delta\Gamma \approx 0.2$, i.e. an approximately 20% net variation in the vortex circulation, reflecting the necessity of maintaining mean blade lift for rotor trim. The results of the simulated sinusoidal variation of the vortex circulation reveal that, if the mean (averaged across the axial span of the ensemble) circulation is kept approximately constant and equal to that of the baseline vortex, there is only a slight influence on the vortex modification effectiveness and efficiency parameters. Further, what little effect is shown is more of a consequence of the "even" and "odd" nature of the wave number, M, rather than the wavelength of the periodic circulation variation. In Fig. 17 "odd" wave numbers have a slight beneficial influence. This wave number influence, though, is anticipated to disappear with increasing axial span of ensemble used in the effectiveness and efficiency parameter estimation. If the vortex circulation is not preserved, but on average shows a net reduction as compared to the baseline vortex than it is anticipated that greater values for the effectiveness and efficiency parameters would result. Further, periodically varying the vortex circulation can be anticipated to influence not the vortex characteristics such as core size and maximum tangential velocity (as studied, in part, herein this paper) but will also strongly influence blade-miss-distance. Reported instances of noise/vibration reduction using active blade control to periodically varying blade circulation, on the basis of this analysis, likely derive the majority of the observed benefits from adjusting the blade-miss-distance rather than some fundamental change in the vortex core characteristics.

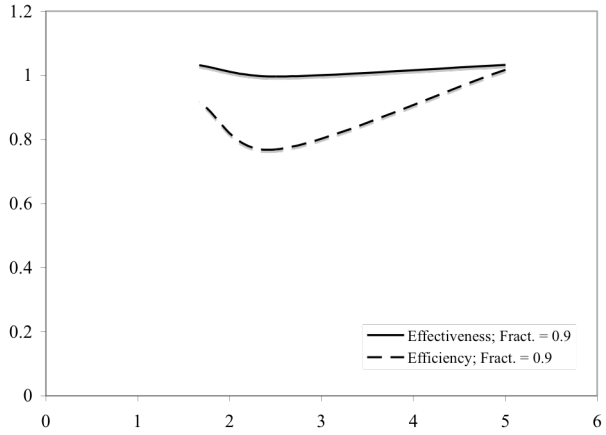

Fig. 17 – Effectiveness and Efficiency of Vortex Modification via Periodic Variation in Vortex Filament Circulation

The above results represent only a preliminary investigation of various different strategies, and resulting estimates of effectiveness and efficiency, for "bulk property" vortical flow modification of line vortices. The next section will discuss the possibility of "destabilizing" the vortex. Such "destabilization" can notionally occur for both baseline/unmodified and modified (such as those studies in the above discussion) vortices. Because of the necessity for brevity only a limited study is performed of the potential of vortex destabilization fro the case of a vortex filament being subjected to a single ideal cut.

D. Vortex Modification via "Destabilization"

Figure 18 illustrates a localized region of flow wherein tangential "disturbance velocity" features, $\hat{v}_\theta^\bullet$, (given short-wavelength excitation) can be observed emerging from the basic flow for the case of a vortex filament with a single ideal cut. The following discussion related to disturbance velocity predictions -- and the corresponding implications for destabilizing the vortex -- for modified or disrupted vortical flow builds off of the approximate analysis presented in the Appendix. These localized disturbance velocity features exhibit "short-wavelength" increases and decreases in strength, as represented by varying the parameter Ω in Fig. 18. These disturbance velocity flow features are not revealed in the basic flow analytical solution for the vortex filaments (Ref. 12). Consequently, the appearance and persistence of these small-scale features can be considered indicative of the general axisymmetric flow stability of these vortex filaments during a portion of their overall evolution with time. Though the dominant "disturbance velocity" flow features observed are the swirling flow fluctuations noted in the intermediate region between vortex breakpoints, there are correspondingly some (comparatively minor) fluctuations in the radial and axial velocities, $\hat{v}_r^\bullet$ and $\hat{v}_z^\bullet$. The Fig. 18 contour plots are presented for $t^\bullet = 0.1$, with short-wavelength excitation where $\Omega = \omega_n t^\bullet = \omega_m t^\bullet = 0$, $\varphi_{mn} = 0$, $a_n = 0.0001$, and $b_n = 0.1$. The tangential disturbance velocity fluctuations predicted are extremely sensitive to the value specified for the parameter a_n, the nth mode amplitude (refer to the Appendix for details). This, in fact, limits the magnitude of a_n to small values, otherwise unrealistically steep (near-singular) gradients for the tangential disturbance velocities. Additional steps, as detailed in the Appendix, are also required to avoid near-singular behavior of the disturbance velocities.

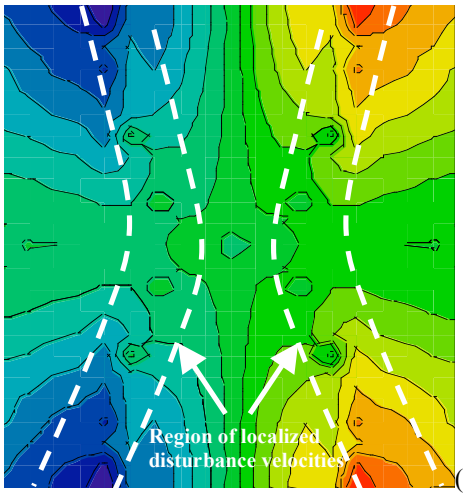

$(\Omega = 0)$

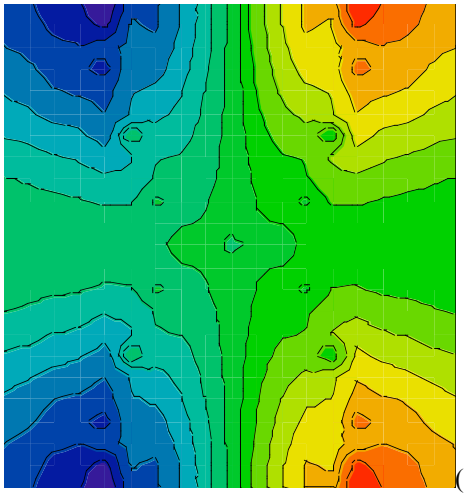

$(\Omega = \pi/3)$

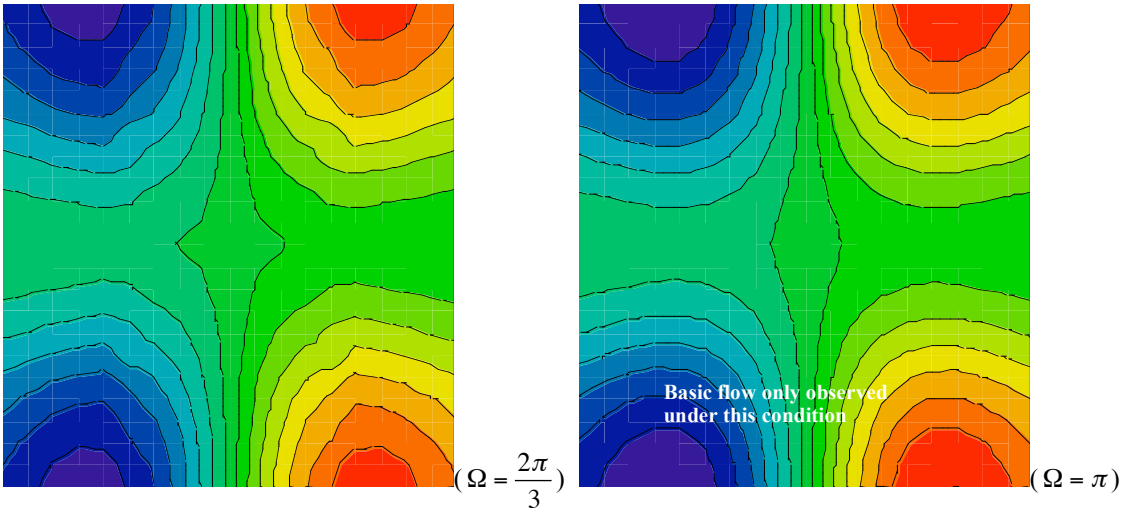

Fig. 18 – Manifestation of Fluctuating Swirling Flow in Vortex Filament Intermediate Region, for a Single Ideal Cut and "parabolic" core ($t^{\bullet} = 0.1$)

Figures 19 and 20 show the influence of "linear mode" (versus "exponential" mode) excitation on the representative case of a vortex filament with a single ideal cut. As discussed in the Appendix, the vortical flow response to such linear modes is linearly proportional to the external excitation amplitudes. Very strong, localized gradients of both axisymmetric and asymmetric distributions of disturbance velocity components are observed in Figs. 19 and 20. Though the overall vortical flow response is time dependent (particularly at very small values of nondimensional time), refer to Fig. 21, in general such flow response cannot be characterized as being an instability in the classic sense as the growth of the disturbance velocities with time is not unbounded. (Note that the top-of-center "breaks" observed in the azimuthal distribution are visualization software artifacts; this fact being highlighted for one of the distributions.)

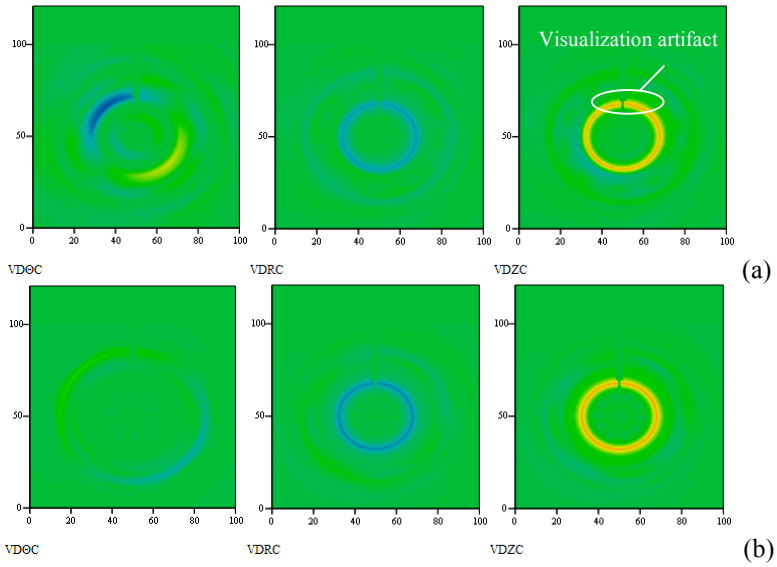

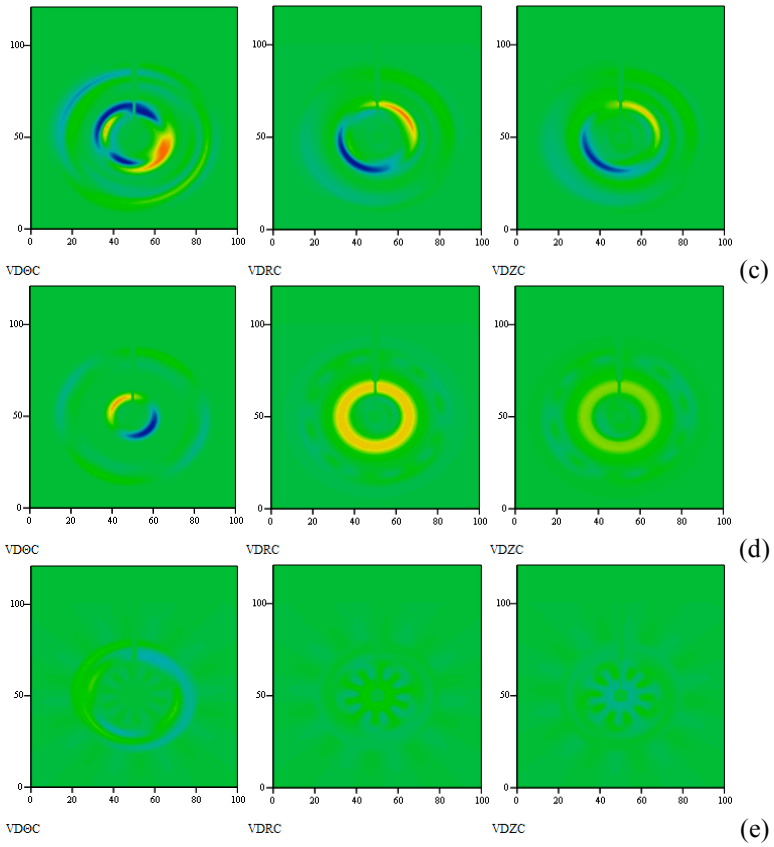

Fig. 19 – Disturbance Velocity Distributions ($t^{\bullet} = 0.1$ and $\Omega = 0$): (a) $z^{\bullet} = 2.2$, (b) $z^{\bullet} = 2$, (c) $z^{\bullet} = 1.4$, (d) $z^{\bullet} = 1$, and (e) $z^{\bullet} = 0$

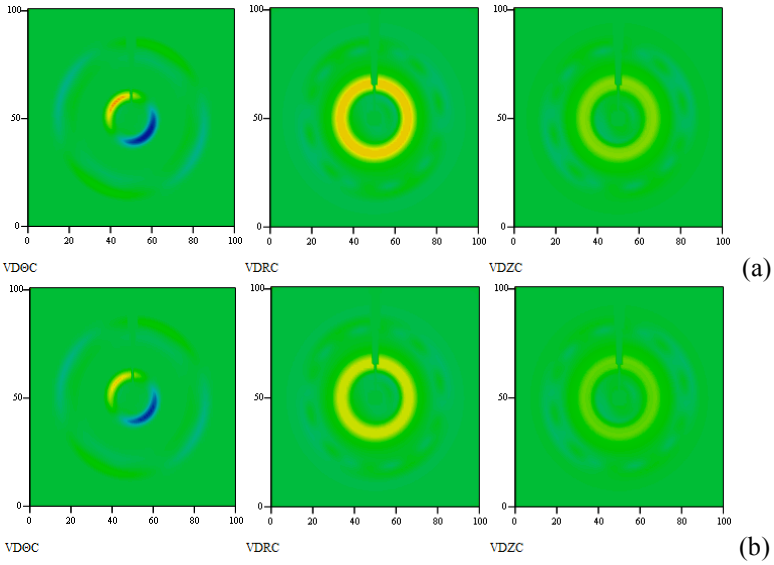

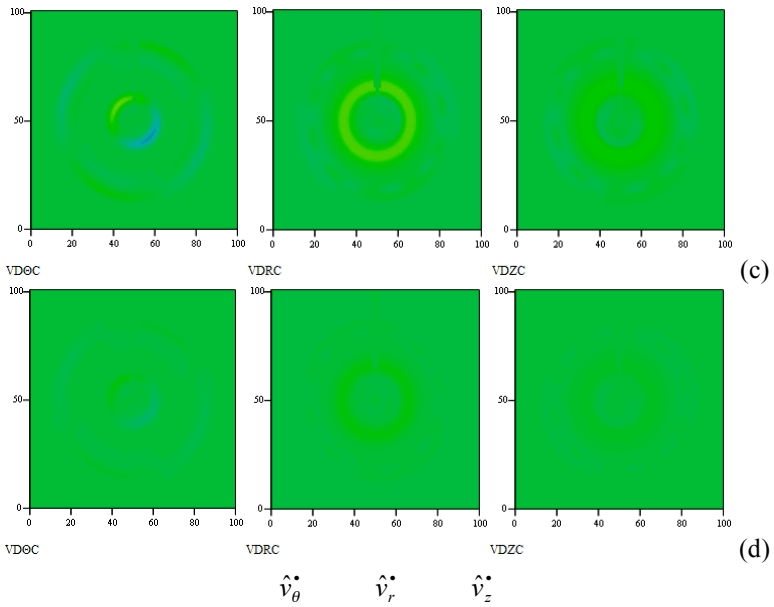

Fig. 20 – Disturbance Velocity Distributions ($z^\bullet = 1$):(a) $\theta = 0,\ 2\pi$, (b) $\theta = \pi/4,\ 7\pi/4$, (c) $\theta = \pi/2,\ 3\pi/2$, (d), $\theta = 3\pi/4,\ 5\pi/4$

Given these predictions of significant disturbance velocities permeating the vortical flow, the question arises as to whether these disturbances are unbounded with time, and therefore reflect a true instability being manifested in the flow, or are the disturbance velocities sufficiently damped or neutral so as not to radically influence the global structure of the vortical flow. Figure 21 presents results for a global disturbance parameter, ϑ , based on the analysis presented in the Appendix, as a function of time that seeks to address this question in a preliminary sense. As can be seen in Fig. 21 the disturbance parameter, ϑ , trend results, with respect to nondimensional, time are not easily to interpret. (Again, Fig. 21 presents preliminary results for the disturbance parameter, ϑ , for the specific case of a vortex filament with a single ideal cut.) Though there is a time dependency of the disturbance parameter it does not suggest the flow response to be unstable in a classic sense as the response is not unbounded with time. This appears to be true for both "linear" and "exponential" modes. It is important to emphasize, though, the limited scope of this particular investigation as only the single ideal cut case was examined versus the other alternate approaches to vortex modification/disruption noted earlier in the paper.

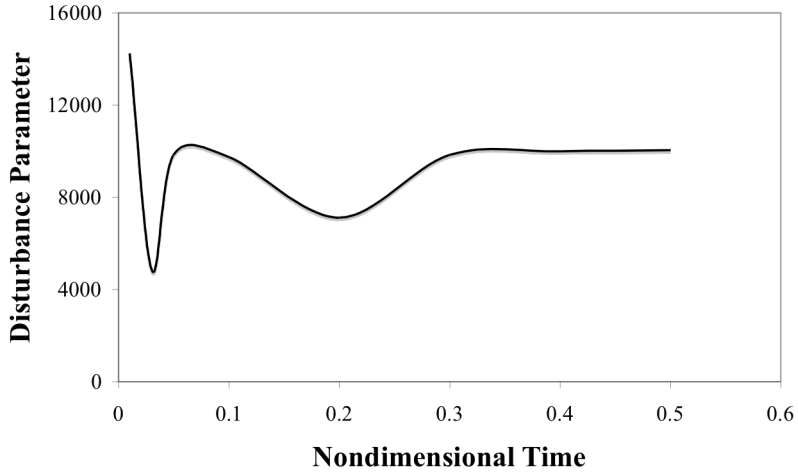

Fig. 21 – Disturbance Parameter Trend with Nondimensional Time (Single Vortex Filament "Ideal Cut," $s/r_{c0} = 1$)

The analysis in the Appendix can be considered as a major advance in the understanding of the time evolution of vortices being subjected to major disruption and/or modification. Previous basic flow analytical solutions (Refs. 10-12), although unsteady in nature, were not intended to predict these disturbance velocity components.

Concluding Remarks

Analytical solutions for the unsteady flow behavior of vortices being subjected to three different types of vortical flow disruption – vortex filament cutting, injection of negative vorticity into the inner vortex core, and periodic changes to the vortex circulation – have been detailed in this paper. This work builds upon previous analytical investigations that have examined the role of initial vorticity distributions on the vortex reconnection and breakdown phenomena. Most importantly, the paper discusses the relevance of the presented analytical work with respect to ongoing efforts by many researchers in the field to develop active control/dissipation of vortical structures – such as trying to enhance the decay of trailed wing-tip vortices of large commercial aircraft to minimize the occurrence of wake upset for such aircraft or, alternatively, modification or dissipation of rotorcraft blade tip vortices to minimize the adverse effects of blade vortex interaction.

Among the key questions raised in this study is what are the proper metrics or parameters needed to define and measure "success" in vortical flow control. Two such metrics are proposed in this paper. These metrics consider the "effectiveness" and "efficiency" of vortex modification while intrinsically accounting for the "extent" and "persistence" of such modification.

Vortex modification, as suggested by this line vortex analysis, seems to be best effected by means of the combined application of vortex filament "cutting" or "breaking" and insertion/injection of negative vorticity into the vortex inner core. Such combined application of vortex "bulk property" vortical flow control is predicted to yield significant reductions in localized vortex kinetic energy so as to potentially significantly moderate body/blade-vortex interactions and, therefore, effecting noise, vibration, and load reduction for rotary-wing platforms.

Finally, a hypothesis, and associated approximate analytical treatment, is advanced wherein vortex filament "destabilization" can be studied. An example analysis case is presented. Both axisymmetric and asymmetric vortical flow (a.k.a "linear" and "exponential") modes are revealed in the resulting three-dimensional flow analysis. In the example provided, the predicted disturbance velocities remain bounded with time and, therefore, do not exhibit classic flow instability. Left to future work, though, is the question of the interdependence between such metrics as the presented "disturbance parameter" and some desired vortical flow end-state.

The work in this paper is preliminary in nature, but, nonetheless, it is anticipated to provide meaningful insight into the development of future active vortical flow control devices/actuators.

References

[1]Kantha, H.L., Lewellen, W.S., and Durgin, F.H., "Response of a Trailing Vortex to Axial Injection into the Core," Journal of Aircraft, Vol. 9, No. 3.

[2]Vasilescu, R. and Dancila, D.S., "Rotor Wake Modifications in Hover using Unsteady Spanwise Blowing," AIAA 2006-1065, 44th AIAA Aerospace Sciences Meeting, Reno, NV, January 9-12, 2006.

[3]Liu, Z., Sankar, L.N., and Hassan, A.A., "Alteration of the Tip Vortex Structure of a Hovering Rotor using Oscillatory Jet Excitation," AIAA 2000-0259, 38th AIAA Aerospace Sciences Meeting, Reno, NV, January 10-13, 2000.

[4]Liu, Z., Sankar, L.N., and Hassan, A.A., "Alteration of the Tip Vortex Structure of a Hovering Rotor by Blowing," AIAA 99-0906, 37th AIAA Aerospace Sciences Meeting, Reno, NV, January 11-14, 1999.

[5]Ash, R.L., Riester, J.E., and Bandyopadhyay, P.R., "A Device for Introducing Helical Perturbations into a Trailing Line Vortex," AIAA 90-1627, AIAA 21st Fluid Dynamics, Plasma Dynamics, and Lasers Conference, Seattle, WA, June 18-20, 1990.

[6]Russell, J.W., Sankar, L.N., Tung, C., and Patterson, M.T., "Alterations of the Tip Vortex Structure from a Hovering Rotor using Passive Tip Devices," 53rd Annual Forum of the American Helicopter Society, Virginia Beach, VA, April 29-May 1, 1997.

[7]Squires, H.B. "The Growth of a Vortex in Turbulent Flow," Aeronautical Quarterly, Vol. 16, August 1965, pp. 302-306.

[8]Bhagwat, M.J. and Leishman, J.G., "Generalized Viscous Vortex Core Models for Application to Free-Vortex Wake and Aeroacoustic Calculations," Proceedings of the 58th Annual Forum of the American Helicopter Society International, Montréal, Canada, June 11-13, 2002.

[9]Batchelor, G.K., "Axial Flow in Trailing Line Vortices," J. Fluid Mech., Vol. 20, Part 4, 1964, pp. 645-658.

[10]Young, L.A., "Vortex Flow Behavior Subsequent to Perpendicular Collision with a Solid Body," Soon to be published NASA TM.

[11]Young, L.A., "Influence of Initial Vorticity Distribution on Axisymmetric Vortex Breakdown and Reconnection," AIAA-2007-1283, AIAA Aerospace Sciences Meeting, Reno, NV, January 8-11, 2006.

[12]Young, L.A., "A Family of Vortices to Study Axisymmetric Vortex Breakdown and Reconnection," 25th AIAA Applied Aerodynamics Conference, Miami, FL, June 25-28, 2007.

[13]Carslaw, H.S. and Jaeger, J.C., Conduction of Heat in Solids, Second Edition, Clarendon Press, Oxford, 1959.

[14]Lamb, H., Hydrodynamics, Sixth Edition, Dover Publications, New York.

[15]White, F.M., *Viscous Fluid Flow,* McGraw-Hill, 1974.

[16]Riahi, D.N., *Flow Instability*, WIT Press, 2000.

[17]López, G., *Partial Differential Equations of First Order and Their Applications to Physics*, World Scientific, Publishing Co. Singapore, 1999.

Appendix – "Disturbance Velocity" Analysis

The bulk of this paper considers the question of whether or not one of four general classes of vortex filament disruption can significantly modify a vortex for some finite period of time such that the net effective kinetic energy of the vortex is reduced below that of the baseline unmodified/undisrupted vortex. Such a transitory reduction in vortex kinetic energy is hypothesized to have potentially a positive influence on a variety of rotary- and fixed-wing flow phenomena, including blade-vortex interaction. But most of this preceding analysis focused on the unsteady basic flow characteristics of the disrupted vortices and did not examine the overall stability characteristics of the flow. The question unanswered is whether or not flow instabilities can be manifested as a result of the vortex disruptions such that the flow state of the destabilized vortex is beneficially predisposed to even further reductions in vortex kinetic energy than the flow state associated with the basic flow solution of the vortex.

The analysis presented in this appendix examines the flow stability of the vortical flow associated with the four vortex modification/strategies examined in the main body of the paper. Intrinsic to the analysis is a reinterpretation of the basic flow solution for the azimuthal vorticity production/dissipation mechanisms for the vortex reconnection problem. The earlier work of Ref. 12 would suggest that the basic flow solution for the azimuthal vorticity component, stemming from consideration of the viscous Helmholtz vorticity transport equation, was only approximate in nature, even with making the a large Reynolds number assumption for the flow. Though this is still the case for the basic flow solution presented, it did suggest that perhaps that the reason that solution did not fully satisfy the azimuthal vorticity transport equation was primarily a consequence of not modeling quasi-periodic (short-wavelength) disturbance velocities, particularly that of the tangential velocity component. Therefore, the Ref. 12 basic flow solution, in this reinterpretation, could be considered an incomplete rather than approximate solution. By formulating the flow problem to consider disturbance velocity components to the basic flow, a more complete (though still restricted to the large Reynolds number assumption) solution/analysis might be derived. This new interpretation of the problem can be seen as fluctuations, as manifested by the disturbance velocities, between two different flow states as represented between proportionality and non-proportionality between the azimuthal vorticity and the tangential velocity distributions. The following analysis not only strives to derive such a more complete solution but also, as a consequence, yields a flow

stability analytical model that addresses the question of flow destabilization as a direct result of the four general classes of vortex disruption/modification studied initially in the context of the basic flow solution.

Revisiting the Helmholtz vorticity transport equation

$$\frac{D\boldsymbol{\omega}}{Dt} = (\boldsymbol{\omega}\cdot\nabla)\mathbf{V} + \nu\nabla^2\boldsymbol{\omega}$$

Which expands out to the cylindrical coordinate system form

$$\frac{\partial\omega_z}{\partial t} + v_r\frac{\partial\omega_z}{\partial r} + \frac{v_\theta}{r}\frac{\partial\omega_z}{\partial\theta} + v_z\frac{\partial\omega_z}{\partial z} =$$
$$\omega_r\frac{\partial v_z}{\partial r} + \frac{\omega_\theta}{r}\frac{\partial v_z}{\partial\theta} + \omega_z\frac{\partial v_z}{\partial z} + \nu\left\{\frac{\partial^2\omega_z}{\partial r^2} + \frac{1}{r}\frac{\partial\omega_z}{\partial r} + \frac{1}{r^2}\frac{\partial^2\omega_z}{\partial\theta^2} + \frac{\partial^2\omega_z}{\partial z^2}\right\}$$

$$\frac{\partial\omega_r}{\partial t} + v_r\frac{\partial\omega_r}{\partial r} + \frac{v_\theta}{r}\frac{\partial\omega_r}{\partial\theta} + v_z\frac{\partial\omega_r}{\partial z} =$$
$$\omega_r\frac{\partial v_r}{\partial r} + \frac{\omega_\theta}{r}\frac{\partial v_r}{\partial\theta} + \omega_z\frac{\partial v_r}{\partial z} + \nu\left\{\frac{\partial^2\omega_r}{\partial r^2} + \frac{1}{r}\frac{\partial\omega_r}{\partial r} + \frac{1}{r^2}\frac{\partial^2\omega_r}{\partial\theta^2} + \frac{\partial^2\omega_r}{\partial z^2}\right\}$$

$$\frac{\partial\omega_\theta}{\partial t} + v_r\frac{\partial\omega_\theta}{\partial r} + \frac{v_\theta}{r}\frac{\partial\omega_\theta}{\partial\theta} + v_z\frac{\partial\omega_\theta}{\partial z} =$$
$$\omega_r\frac{\partial v_\theta}{\partial r} + \frac{\omega_\theta}{r}\frac{\partial v_\theta}{\partial\theta} + \omega_z\frac{\partial v_\theta}{\partial z} + \nu\left\{\frac{\partial^2\omega_\theta}{\partial r^2} + \frac{1}{r}\frac{\partial\omega_\theta}{\partial r} + \frac{1}{r^2}\frac{\partial^2\omega_\theta}{\partial\theta^2} + \frac{\partial^2\omega_\theta}{\partial z^2}\right\}$$

(8a-c)

Previous work would show that only stable solutions exist for the heat conduction equation (e.g. Ref. 13). Therefore, there should be no vortical flow instabilities with respect to the vortex filament axial vorticity and tangential velocity components. Further, as the radial vorticity solution nearly satisfies the heat conduction equation, it is unlikely that flow instabilities would be principally manifested as a consequence of the radial vorticity distribution. There remains, however, the possibility that flow instabilities could be manifested in those portions of the flow dominated by the azimuthal vorticity. This possibility will be examined more closely next.

Equation 8c is simplified by first applying θ–symmetry and then being nondimensionalized.

$$v_r^\bullet\frac{\partial\omega_\theta^\bullet}{\partial r^\bullet} + v_z^\bullet\frac{\partial\omega_\theta^\bullet}{\partial z^\bullet} = \omega_r^\bullet\frac{\partial v_\theta^\bullet}{\partial r^\bullet} + \omega_z^\bullet\frac{\partial v_\theta^\bullet}{\partial z^\bullet} + \frac{1}{\mathrm{Re}}\left\{\frac{\partial^2\omega_\theta^\bullet}{\partial\left(r^\bullet\right)^2} + \frac{1}{r^\bullet}\frac{\partial\omega_\theta^\bullet}{\partial r^\bullet} + \frac{\partial^2\omega_\theta^\bullet}{\partial\left(z^\bullet\right)^2} - \frac{\partial\omega_\theta^\bullet}{\partial t^\bullet}\right\} \tag{9}$$

Making, as noted in Ref. 12, the large Reynolds number assumption, Eq. 9 reduces to

$$v_r^\bullet\frac{\partial\omega_\theta^\bullet}{\partial r^\bullet} + v_z^\bullet\frac{\partial\omega_\theta^\bullet}{\partial z^\bullet} \approx \omega_r^\bullet\frac{\partial v_\theta^\bullet}{\partial r^\bullet} + \omega_z^\bullet\frac{\partial v_\theta^\bullet}{\partial z^\bullet} \tag{10}$$

Next, the velocity can be expressed as follows in terms of both an undisturbed, but unsteady, velocity solutions (defined in terms of v_r, v_θ, and v_z velocity components) and disturbance velocity components defined as in a similar manner to classic fluid flow stability theory, e.g. Refs. 15-16, by $\hat{v}_r$, $\hat{v}_\theta$, and $\hat{v}_z$.

$$\mathbf{V} = \begin{bmatrix} v_r + \hat{v}_r & v_\theta + \hat{v}_\theta & v_z + \hat{v}_z \end{bmatrix}$$

In turn, that also implies (principally as a consequence of the length-scale factor methodology relating the axial and radial vorticity to the axial and radial velocity components) that the vorticity can be similarly expressed in terms of both undisturbed, by unsteady, solution and disturbance vorticity components.

$$\boldsymbol{\omega} = \begin{bmatrix} \omega_r + \hat{\omega}_r & \omega_\theta + \hat{\omega}_\theta & \omega_z + \hat{\omega}_z \end{bmatrix}$$

Substitution of the above disturbance expressions for the vorticity into the Helmholtz equations gives

$$\left(v_r^\bullet + \hat{v}_r^\bullet\right)\left(\frac{\partial \omega_\theta^\bullet}{\partial r^\bullet} + \frac{\partial \hat{\omega}_\theta^\bullet}{\partial r^\bullet}\right) + \left(v_z^\bullet + \hat{v}_z^\bullet\right)\left(\frac{\partial \omega_\theta^\bullet}{\partial z^\bullet} + \frac{\partial \hat{\omega}_\theta^\bullet}{\partial z^\bullet}\right) = \left(\omega_r^\bullet + \hat{\omega}_r^\bullet\right)\left(\frac{\partial v_\theta^\bullet}{\partial r^\bullet} + \frac{\partial \hat{v}_\theta^\bullet}{\partial r^\bullet}\right) + \left(\omega_z^\bullet + \hat{\omega}_z^\bullet\right)\left(\frac{\partial v_\theta^\bullet}{\partial z^\bullet} + \frac{\partial \hat{v}_\theta^\bullet}{\partial z^\bullet}\right)$$

(11)

Next, in a similar manner as is done for classic stability theory, the basic flow (undisturbed and known) terms of Eq. 11 are subtracted out. Consequently, the following approximate disturbance equation can be derived.

$$\begin{aligned} & v_r^\bullet \frac{\partial \hat{\omega}_\theta^\bullet}{\partial r^\bullet} + v_z^\bullet \frac{\partial \hat{\omega}_\theta^\bullet}{\partial z^\bullet} - \omega_r^\bullet \frac{\partial \hat{v}_\theta^\bullet}{\partial r^\bullet} - \omega_z^\bullet \frac{\partial \hat{v}_\theta^\bullet}{\partial z^\bullet} \\ & + \hat{v}_r^\bullet \frac{\partial \omega_\theta^\bullet}{\partial r^\bullet} + \hat{v}_z^\bullet \frac{\partial \omega_\theta^\bullet}{\partial z^\bullet} - \hat{\omega}_r^\bullet \frac{\partial v_\theta^\bullet}{\partial r^\bullet} - \hat{\omega}_z^\bullet \frac{\partial v_\theta^\bullet}{\partial z^\bullet} \\ & + \hat{v}_r^\bullet \frac{\partial \hat{\omega}_\theta^\bullet}{\partial r^\bullet} + \hat{v}_z^\bullet \frac{\partial \hat{\omega}_\theta^\bullet}{\partial z^\bullet} - \hat{\omega}_r^\bullet \frac{\partial \hat{v}_\theta^\bullet}{\partial r^\bullet} - \hat{\omega}_z^\bullet \frac{\partial \hat{v}_\theta^\bullet}{\partial z^\bullet} \approx 0 \end{aligned}$$

(12a-c)

Implied in the previously applied length scale factor methodology

$$v_z = -\ell \omega_z \qquad v_r = -\ell \omega_r$$

And

$$\hat{v}_z = -\ell \hat{\omega}_z \qquad \hat{v}_r = -\ell \hat{\omega}_r$$

(13a-d)

However, in the case of the tangential velocity and vorticity components, it can be assumed to follow that

$$v_\theta \neq -\ell \omega_\theta$$

As noted above, the tangential velocity for the basic flow is not, in general, dependent upon the azimuthal vorticity, particularly for $t \to 0$, within the range $-\ell \le z \le \ell$. But, however, for the tangential disturbance velocities it is assumed that

$$\hat{v}_\theta = -\ell \hat{\omega}_\theta$$

(14a-b)

Note the following nondimensionalization of the length scale factor: $\ell^{\bullet} = \ell / r_{c0A}$. Note, further, that definition and application of the length-scale factor(s) is dependent upon whether or not the basic flow is locally (axially) symmetrical or nonsymmetrical (as defined in the context of Ref. 12).‡

Making the above substitutions yields

$$\hat{v}_r^{\bullet}\left(\frac{\partial \omega_\theta^{\bullet}}{\partial r^{\bullet}} + \frac{1}{\ell^{\bullet}}\frac{\partial v_\theta^{\bullet}}{\partial r^{\bullet}}\right) + \hat{v}_z^{\bullet}\left(\frac{\partial \omega_\theta^{\bullet}}{\partial z^{\bullet}} + \frac{1}{\ell^{\bullet}}\frac{\partial v_\theta^{\bullet}}{\partial z^{\bullet}}\right) \approx 0 \tag{15}$$

It is important to note that in Eq. 15 basic flow analytical solutions for $\omega_\theta^{\bullet}$ and $v_\theta^{\bullet}$ have been previously derived and reported in Ref. 12; therefore, only $\hat{v}_r^{\bullet}$ and $\hat{v}_z^{\bullet}$ remain to be solved for. The resulting disturbance velocities to some degree can be considered self-excited oscillations between two different flow states (one where $v_\theta / \omega_\theta \neq constant$, i.e. the basic flow, and the other flow state where $v_\theta / \omega_\theta \rightarrow constant$) for regions of flow dominated by azimuthal vorticity. This is analogous to the class of "resonant" type flow instabilities (Ref. 16).

Differentiating the above equation while at the same time relating the disturbance velocity components to each other via the axisymmetric flow continuity equation, $\hat{v}_r^{\bullet} / r^{\bullet} + \partial \hat{v}_r^{\bullet} / \partial r^{\bullet} + \partial \hat{v}_z^{\bullet} / \partial z^{\bullet} = 0$, yields

$$\frac{\partial \hat{v}_r^{\bullet}}{\partial r^{\bullet}} + A\frac{\partial \hat{v}_r^{\bullet}}{\partial z^{\bullet}} + B\hat{v}_r^{\bullet} \approx 0$$

$$\hat{v}_z^{\bullet} = A\hat{v}_r^{\bullet}$$

Where

$$A \equiv -\frac{\left(\ell^{\bullet}\,\partial \omega_\theta^{\bullet} / \partial r^{\bullet} + \partial v_\theta^{\bullet} / \partial r^{\bullet}\right)}{\left(\ell^{\bullet}\,\partial \omega_\theta^{\bullet} / \partial z^{\bullet} + \partial v_\theta^{\bullet} / \partial z^{\bullet}\right)}$$

And

$$B \equiv \frac{1}{r^{\bullet}} + \frac{\partial A}{\partial z^{\bullet}}$$

Or

---

‡ Specifically, local (symmetrical or nonsymmetrical) length scale factors can be defined, more generally, by a length scale function $\ell(\ldots)$, such that

$$\Delta\omega_\theta\left(N, i, \gamma_i, r_{o_i}, a_i, b_i, r, z, t\right) = \ell(N, i, z)\, h\left(\gamma_i, r_{o_i}, a_i, b_i, r, z, t\right)$$

And, further,

$$\omega_\theta = \sum_{i=1}^{N} \Delta\omega_\theta\left(N, i, \gamma_i, r_{o_i}, a_i, b_i, r, z, t\right)$$

Where the function $h(\ldots)$ and the length-scale function, $\ell(\ldots)$, and other associated functions are defined in the Ref. 8 work and can accommodate multiple breakpoints and a wide array of initial vorticity distributions.

$$B = \frac{1}{r^{\bullet}} - \frac{\left(\ell^{\bullet}\,\partial^2\omega_\theta^{\bullet}/\partial r^{\bullet}\partial z^{\bullet} + \partial^2 v_\theta^{\bullet}/\partial r^{\bullet}\partial z^{\bullet}\right)}{\left(\ell^{\bullet}\,\partial\omega_\theta^{\bullet}/\partial z^{\bullet} + \partial v_\theta^{\bullet}/\partial z^{\bullet}\right)} + \frac{\left(\ell^{\bullet}\,\partial\omega_\theta^{\bullet}/\partial r^{\bullet} + \partial v_\theta^{\bullet}/\partial r^{\bullet}\right)\left(\ell^{\bullet}\,\partial^2\omega_\theta^{\bullet}/\partial\left(z^{\bullet}\right)^2 + \partial^2 v_\theta^{\bullet}/\partial\left(z^{\bullet}\right)^2\right)}{\left(\ell^{\bullet}\,\partial\omega_\theta^{\bullet}/\partial z^{\bullet} + \partial v_\theta^{\bullet}/\partial z^{\bullet}\right)^2}$$

(16a-e)

Where A and B are variable coefficients in the above first-order partial differential equation (PDE), e.g. Ref. 17, which are, in turn, based on known analytical solutions for $\omega_\theta^{\bullet}$ and $v_\theta^{\bullet}$. It is an important to note that the use of the axisymmetric form of the continuity equation is not strictly valid. There are anticipated to be periodic azimuthal variation of all three disturbance velocity components. By employing the axisymmetric continuity equation, imposing, in particular, a non-azimuthal-variation of the tangential disturbance velocity results in effective source and sink distributions in the r-z plane for the radial and axial disturbance velocity components. Such sources and sinks for $\hat{v}_r^{\bullet}$ and $\hat{v}_r^{\bullet}$ are periodic in time and out of phase with $v_\theta^{\bullet}$ variation. Further, this dictates the emergence of regions of very steep gradients in all three disturbance velocity components. This inviscid-like source and sink flow behavior is only a "pseudo-axisymmetric" approximation of the true vortical flow. However, as will be seen later, from this initial formulation of the problem, an asymmetric extension of the approximate solution can be derived that more closely represents the actual physical flow.

Given Eq. 16a-e, a solution for the disturbance azimuthal vorticity and tangential velocity can be derived, i.e.

$$\hat{\omega}_\theta^{\bullet} = \frac{\partial\hat{v}_r^{\bullet}}{\partial z^{\bullet}} - \frac{\partial\hat{v}_z^{\bullet}}{\partial r^{\bullet}}$$

And

$$\hat{v}_\theta^{\bullet} = \ell^{\bullet}\left(\frac{\partial\hat{v}_z^{\bullet}}{\partial r^{\bullet}} - \frac{\partial\hat{v}_r^{\bullet}}{\partial z^{\bullet}}\right)$$

(17a-b)

At this point, the analysis of this paper departs somewhat from classic linear flow stability theory (i.e. assuming periodic infinitesimal excitation and decomposing the disturbance equation into a linear system which can then be studied by a variety of stability analysis techniques) and an alternative approach is presented in which it is attempted to approximately, though directly, solve for the disturbance velocities.

The intent of the following analysis is to derive an approximation to Eq. 16 that allows the first order partial differential equation to become quasi-separable and then solve accordingly. The first step in effecting the required approximation is to note the observation $A \propto 1/r^{\bullet}$ for $r^{\bullet} \to 0$ and the region $\left|z^{\bullet}\right| \le z_w^{\bullet}$ (assuming a single ideal cut or other vortex filament disruption). This can be approximately for two discrete regions within $\left|z^{\bullet}\right| \le z_w^{\bullet}$: an azimuthal vorticity dominated region ($1 \le \left|z^{\bullet}\right| \le z_w^{\bullet}$) where the basic flow solution has a singularity at the centerline of the vortex filament (as demonstrated in Ref. 10) and the tangential velocity dominated region ($\left|z^{\bullet}\right| \le 1$). For the azimuthal vorticity dominated region, $\omega_\theta^{\bullet} \to f\left(z^{\bullet}\right)/r^{\bullet}$ as $r^{\bullet} \to 0$ and, further, $\left|\omega_\theta^{\bullet}\right| >> \left|v_\theta^{\bullet}\right|$. In this first case,

$A \to -\left(\partial\omega_\theta^\bullet/\partial r^\bullet\right)\Big/\left(\partial\omega_\theta^\bullet/\partial z^\bullet\right) \to -\left(-f\left(z^\bullet\right)\Big/\left(r^\bullet\right)^2\right)\Big/\left(\left(\partial f/\partial z^\bullet\right)\Big/r^\bullet\right) \to \left(1/r^\bullet\right)\left(f\Big/\left(\partial f/\partial z^\bullet\right)\right)$ and so as asserted $A \propto 1/r^\bullet$. For tangential velocity dominated regions, $v_\theta^\bullet \to g\left(z^\bullet\right)r^\bullet$ as $r^\bullet \to 0$ and as $\left|\omega_\theta^\bullet\right| \to 0$. For the second case $A \to -\left(\partial v_\theta^\bullet/\partial r^\bullet\right)\Big/\left(\partial v_\theta^\bullet/\partial z^\bullet\right) \to -g\left(z^\bullet\right)\Big/\left(\left(\partial g/\partial z^\bullet\right)r^\bullet\right) \to \left(-1/r^\bullet\right)\left(g\Big/\left(\partial g/\partial z^\bullet\right)\right)$. The consequence of these observations is that Eq. 16a can be considered somewhat independently for the two identified flow regions.

$$\frac{\partial\hat{v}_r^\bullet}{\partial r^\bullet} + A\frac{\partial\hat{v}_r^\bullet}{\partial z^\bullet} + B\hat{v}_r^\bullet \approx 0$$

$$\downarrow$$

$$\frac{\partial\hat{v}_r^\bullet}{\partial r^\bullet} + A\frac{\partial\hat{v}_r^\bullet}{\partial z^\bullet} + \left(\frac{1}{r^\bullet} + \frac{\partial A}{\partial z^\bullet}\right)\hat{v}_r^\bullet \approx 0 \qquad (18)$$

This equation must be subject to the following boundary conditions.

$$\hat{v}_r^\bullet = 0 \quad \text{For} \qquad r^\bullet = 0$$

$$\hat{v}_\theta^\bullet = 0 \quad \text{For} \qquad r^\bullet = 0$$

$$\hat{v}_z^\bullet = 0 \quad \text{For} \qquad \left|z^\bullet\right| = z_w^\bullet$$

$$\hat{v}_r^\bullet \to \hat{v}_z^\bullet \to \hat{v}_\theta^\bullet \to 0 \qquad \text{For} \qquad r^\bullet \to \infty$$

$$\left|\partial\hat{v}_\theta^\bullet/\partial z^\bullet\right| << \infty \quad \text{For} \qquad \left|z^\bullet\right| = z_w^\bullet \qquad (19a\text{-}e)$$

The first two boundary conditions are critical. They are especially difficult to satisfy, as the basic flow azimuthal vorticity solution has a singularity at $r^\bullet = 0$ for those regions of the flow seeing significant azimuthal vorticity production.

For regions of flow near the local plane of symmetry -- in this case of a single ideal vortex filament cut, $z^\bullet = 0$ -- $A \to 0$ as $r^\bullet = 0$ for small values of nondimensional time. Or, more specifically, a cutoff condition, $A\big|_{r\to 0^+} < \alpha$, can be applied to the disturbance equation such that the following holds

$$\frac{\partial\hat{v}_r^\bullet}{\partial r^\bullet} + A\frac{\partial\hat{v}_r^\bullet}{\partial z^\bullet} + \left(\frac{1}{r^\bullet} + \frac{\partial A}{\partial z^\bullet}\right)\hat{v}_r^\bullet \approx 0$$

$$\downarrow$$

$$\frac{\partial\hat{v}_r^\bullet}{\partial r^\bullet} + \frac{\hat{v}_r^\bullet}{r^\bullet} \approx 0 \qquad (20)$$

Which has only two solutions

$$\hat{v}_r^\bullet \propto 1/r^\bullet \qquad \text{Or} \qquad \hat{v}_r^\bullet = 0 \qquad (21)$$

The first solution violates the boundary conditions noted above -- specifically, $\hat{v}_r^\bullet = 0$ at $r^\bullet = 0$ for all $z^\bullet$ and $t^\bullet$. Therefore, the second solution must be the valid solution for the discrete regions (axially) of flow where $A \to 0$ as $r^\bullet = 0$, or alternatively $A\big|_{r\to 0^+} < \alpha$.

Assume a quasi-separable function form of the radial disturbance velocity such that $\hat{v}_r^\bullet = f\left(r^\bullet\right)g(A)$ and, correspondingly, $g(A) = h\left(r^\bullet, z^\bullet, t^\bullet\right) \approx \lambda\left(r^\bullet\right)k\left(z^\bullet, t^\bullet\right)$, where from the earlier functional analysis discussion $\lambda\left(r^\bullet\right) \approx 1/r^\bullet$ and $k\left(z^\bullet, t^\bullet\right) \approx O(1)$. Therefore

$$\frac{\partial \hat{v}_r^\bullet}{\partial r^\bullet} + A\frac{\partial \hat{v}_r^\bullet}{\partial z^\bullet} + \left(\frac{1}{r^\bullet} + \frac{\partial A}{\partial z^\bullet}\right)\hat{v}_r^\bullet \approx 0$$

$$\downarrow$$

$$g\frac{\partial f}{\partial r^\bullet} + f\frac{\partial g}{\partial r^\bullet} + Af\frac{\partial g}{\partial z^\bullet} + \left(\frac{1}{r^\bullet} + \frac{\partial A}{\partial z^\bullet}\right)fg \approx 0$$

$$\downarrow$$

$$\frac{1}{f}\frac{\partial f}{\partial r^\bullet} + \frac{A}{g}\frac{\partial g}{\partial z^\bullet} + \frac{\partial A}{\partial z^\bullet} + \frac{1}{g}\frac{\partial g}{\partial r^\bullet} + \frac{1}{r^\bullet} \approx 0$$

$$\downarrow$$

$$\frac{1}{f}\frac{\partial f}{\partial r^\bullet} + \frac{A}{g}\frac{\partial g}{\partial z^\bullet} + \frac{\partial A}{\partial z^\bullet} + \left\{\frac{1}{\lambda}\frac{\partial \lambda}{\partial r^\bullet}k\left(z^\bullet, t^\bullet\right) + \frac{1}{r^\bullet}\right\} \approx 0 \qquad (22)$$

Note that when $k\left(z^\bullet, t^\bullet\right) \neq 1$ then the radial and axial disturbance velocities are receiving significant inflow and outflow from the effective sink and source terms (stemming from the "pseudo-axisymmetric" approximation imposed on the problem) fed by the tangential disturbance velocity variation with time.

Equation 22 reduces the problem down to following first-order partial differential equation, which is solvable by the separation of variables method

$$\frac{1}{f}\frac{\partial f}{\partial r^\bullet} + \frac{A}{g}\frac{\partial g}{\partial z^\bullet} + \frac{\partial A}{\partial z^\bullet} \approx 0$$

Where, given the previous functional analysis/discussion

$$\left\{\frac{1}{\lambda}\frac{\partial \lambda}{\partial r^\bullet}k\left(z^\bullet, t^\bullet\right) + \frac{1}{r^\bullet}\right\} \to \left\{r^\bullet\left(-1\Big/\left(r^\bullet\right)^2\right) + \frac{1}{r^\bullet}\right\} \to 0 \qquad (23a\text{-}b)$$

The resulting two ordinary differential equations are

$$\frac{1}{f}\frac{\partial f}{\partial r^\bullet} + b \approx 0$$

$$\downarrow$$

$$f\left(r^\bullet\right) = e^{-br^\bullet}$$

And

$$\frac{A}{g}\frac{\partial g}{\partial z^{\bullet}}+\frac{\partial A}{\partial z^{\bullet}}-b\approx 0$$

$$\downarrow$$

$$g(A)=\frac{a}{A}e^{\int (b/A)dz^{\bullet}}$$

(24a-b)

Therefore, the corresponding solutions to Eq. 16a are

$$\hat{v}_r^{\bullet}\approx\frac{a}{A}e^{-br^{\bullet}+\int (b/A)dz^{\bullet}} \qquad \text{For } 0\le\left|z^{\bullet}\right|\le z_w^{\bullet} \text{ and } A\big|_{r\to 0^+}\ge\alpha$$

$$\hat{v}_r^{\bullet}\approx 0 \qquad \text{For } \left|z^{\bullet}\right|>z_w^{\bullet} \text{ or } A\big|_{r\to 0^+}<\alpha$$

(25a-b)

The "constants," a and b, in Eq. 25a-b are arbitrary functions of time. In keeping with classic flow linear stability analysis, it can be assumed that, in general

$$a=\sum_{n=1}^{\infty}a_n\left(1+\cos\omega_n t^{\bullet}\right) \qquad \text{And} \qquad b=1+\sum_{m=1}^{\infty}b_m\cos\left(\omega_m t^{\bullet}+\phi_{mn}\right)$$

Or, as studied in this paper, a simpler two-mode formulation of $a=a_1\left(1+\cos\omega_1 t^{\bullet}\right)$ and $b=1+b_2\cos\left(\omega_2 t^{\bullet}+\phi_{21}\right)$ is employed. In this case a_n, b_m, ω_n, and ω_m are the (nth and mth) modal amplitudes and frequencies of interest. Additionally, ϕ_{mn} is the phase angle offset for the mth mode with respect to the nth mode. Two observations should be noted for the quasi-periodic expressions assumed for a and b. First, the predicted fluctuation should be between the basic flow state and a second alternate flow state. Therefore the fluctuations should never result in flow behavior outside of those two flow state extremes; i.e. this can be interpreted as $a\ge 0$ for all $t^{\bullet}$. Second, the quasi-periodic expression for b is consistent with the earlier assumption that $k\left(z^{\bullet},t^{\bullet}\right)\approx O(1)$ if the values of values of a and b are assumed to be typically very small, on the order of $0\le a\le 0.001$ and $0\le b\le 0.1$. (The restriction on b being very small can be relaxed with the above solution being extended from its' "pseudo-axisymmetric" origin and taking on a more asymmetric character by allowing periodic variation of the velocity components along the filament azimuth.) Additionally, it should be noted that there are also important issues regarding the usage of the parameter A as to dealing with (near)-singularities in its estimation. First, a "cutoff" constant, α, has been included in the above equation; typically, as used in this paper, $\alpha\approx 0.01$. Second, as the parameter A (the axial vorticity and tangential velocity "forcing" function) can be expressed as $A=-A_1/A_2$, a nominator and denominator term, refer to Eq. 16c, therefore, consequently, the following "de-singularization" approach can be taken where if $\left|A_1\right|\le\alpha_1$ or $\left|A_2\right|\le\alpha_2$ then, correspondingly, $A_1=\alpha_1 sign\left(A_1\right)$ or $A_2=\alpha_2 sign\left(A_2\right)$ -- where, unless otherwise stated in this paper, $\alpha_1=\alpha_2=0.1$. To reiterate to emphasize the point, the constants α, α_1, and α_2 are somewhat arbitrary in the assignment of their values and are employed solely for the purposes of de-singularizing the solution, Eq. 25a. The primary instability (tangential velocity disturbances) observed in the analysis, for an initially parabolic vorticity distribution with a single ideal cut in the vortex filament, are manifested as clockwise and counter-clockwise rotating toroidal structures of swirling flow axially aligned along, and within, the vortex filament inner core. There are also indications of minor instabilities with respect to the radial and axial disturbance velocities, but these are considerably less sensitive to excitation than the instabilities observed in the tangential velocity profiles.

Substituting Eq. 25a-b into Eqs. 16b and 17b yields, for $0 \le \left|z^{\bullet}\right| \le z_w^{\bullet}$ and $A\big|_{r\to 0^+} \ge \alpha$, solutions for the axial and tangential disturbance velocities.

$$\hat{v}_z^{\bullet} \approx a e^{-br^{\bullet} + \int (b/A) dz^{\bullet}}$$

$$\hat{v}_\theta^{\bullet} = a e^{-br^{\bullet} + \int (b/A) dz^{\bullet}} \left\{ \frac{1}{A^2}\left(\frac{\partial A}{\partial z^{\bullet}} - b\right) - b\left(\int \left(\frac{1}{A^2}\frac{\partial A}{\partial r^{\bullet}}\right) dz^{\bullet} + 1\right)\right\}$$

Or, alternatively, for $\left|z^{\bullet}\right| > z_w^{\bullet}$ or $A\big|_{r\to 0^+} < \alpha$, it is required that

$$\hat{v}_z^{\bullet} \approx 0 \qquad \text{And} \qquad \hat{v}_\theta^{\bullet} \approx 0$$

(26a-d)

As noted before, the above approximate analysis does not incorporate the influence of azimuthal variations in the three disturbance velocity components. One of the consequences of this approximation is the appearance of effective sources and sinks in the r-z plane in the vortical flow. A simple refined-approximation correction can be made to the above expressions to partially account for such azimuthal variations. First, assume that the radial and axial disturbance velocities vary azimuthally, such that

$$\hat{v}_{zc}^{\bullet} = \hat{v}_z^{\bullet} \cos\left(k\theta + \varphi\right)$$
$$\hat{v}_{rc}^{\bullet} = \hat{v}_r^{\bullet} \cos\left(k\theta + \varphi\right)$$

(27a-b)

Applying the full continuity equation, using the above "corrected" radial and axial disturbance velocity expressions gives

$$\frac{v_{rc}^{\bullet}}{r^{\bullet}} + \frac{\partial v_{rc}^{\bullet}}{\partial r^{\bullet}} + \frac{1}{r^{\bullet}}\frac{\partial \hat{v}_{\theta c}^{\bullet}}{\partial \theta} + \frac{\partial \hat{v}_{zc}^{\bullet}}{\partial z^{\bullet}} = 0$$

$$\downarrow$$

$$\hat{v}_{\theta c}^{\bullet} = -\int r^{\bullet}\left(\hat{v}_{rc}^{\bullet}/r^{\bullet} + \partial \hat{v}_{rc}^{\bullet}/\partial r^{\bullet} + \partial \hat{v}_{zc}^{\bullet}/\partial z^{\bullet}\right) d\theta$$

$$\downarrow$$

$$\hat{v}_{\theta c}^{\bullet} = -r^{\bullet}\left(\hat{v}_r^{\bullet}/r^{\bullet} + \partial \hat{v}_r^{\bullet}/\partial r^{\bullet} + \partial \hat{v}_z^{\bullet}/\partial z^{\bullet}\right) \cdot \int \cos\left(k\theta + \varphi\right) d\theta$$

$$\downarrow$$

$$\hat{v}_{\theta c}^{\bullet} = -\frac{1}{k} r^{\bullet}\left(\hat{v}_r^{\bullet}/r^{\bullet} + \partial \hat{v}_r^{\bullet}/\partial r^{\bullet} + \partial \hat{v}_z^{\bullet}/\partial z^{\bullet}\right) \sin\left(k\theta + \varphi\right)$$

(28)

Now the uncorrected and corrected tangential disturbance velocities can be related to each other by the expression

$$\left(\hat{v}_\theta^{\bullet}\right)^2 \approx \frac{1}{2\pi}\int_0^{2\pi} \left(\hat{v}_{\theta c}^{\bullet}\right)^2 d\theta$$

(29)

Substituting Eq. 28 into Eq. 29 yields

$$\left(\hat{v}_\theta^\bullet\right)^2 \approx \frac{1}{2\pi k^3}\left(r^\bullet\right)^2\left(\hat{v}_r^\bullet/r^\bullet + \partial\hat{v}_r^\bullet/\partial r^\bullet + \partial\hat{v}_z^\bullet/\partial z^\bullet\right)^2\left\{\frac{1}{2}\left(k\theta+\varphi\right) - \frac{1}{4}\sin\left(2\left(k\theta+\varphi\right)\right)\Big|_0^{2\pi}\right\}$$

$$\downarrow$$

$$\left(\hat{v}_\theta^\bullet\right)^2 \approx \frac{1}{2\pi k^3}\left(r^\bullet\right)^2\left(\hat{v}_r^\bullet/r^\bullet + \partial\hat{v}_r^\bullet/\partial r^\bullet + \partial\hat{v}_z^\bullet/\partial z^\bullet\right)^2\left\{\pi k + \frac{1}{4}\sin\left(2\varphi\right) - \frac{1}{4}\sin\left(2\left(2\pi k+\varphi\right)\right)\right\}$$

(30)

Given Eqs. 17b and 30, the modal number k can be solved for, recognizing that it is, by definition, an integer, yielding

$$\frac{1}{2\pi k^3}\left(r^\bullet\right)^2\left(\hat{v}_r^\bullet/r^\bullet + \partial\hat{v}_r^\bullet/\partial r^\bullet + \partial\hat{v}_z^\bullet/\partial z^\bullet\right)^2\left\{\pi k + \frac{1}{4}\sin\left(2\varphi\right) - \frac{1}{4}\sin\left(2\left(2\pi k+\varphi\right)\right)\right\} = \left(\partial\hat{v}_z^\bullet/\partial r^\bullet - \partial\hat{v}_r^\bullet/\partial z^\bullet\right)^2$$

(31)

Let the following parameter be defined

$$x = \frac{r^\bullet}{\sqrt{2}}\left|\left(\hat{v}_r^\bullet/r^\bullet + \partial\hat{v}_r^\bullet/\partial r^\bullet + \partial\hat{v}_z^\bullet/\partial z^\bullet\right)\Big/\left(\partial\hat{v}_z^\bullet/\partial r^\bullet - \partial\hat{v}_r^\bullet/\partial z^\bullet\right)\right|$$

(32)

Then the effective modal number and phase angle, k and φ, can be solved for, given Eqs. 31 and 32, when recognizing that k is an integer and the phase angle offset is a small value.

$$k \approx \left[x\right] \qquad \text{If} \qquad \left[x\right] \le K_{\max}$$

$$k = K_{\max} \qquad \text{If} \qquad \left[x\right] > K_{\max}$$

And

$$y \approx 4\pi k\left(\left(k/x\right)^2 - 1\right)$$

$$\varphi \approx \frac{1}{2}\,\text{asin}\left(y\right) \qquad \text{If } |y| \le 1$$

$$\varphi \approx \frac{\pi}{4}\,\text{sign}\left(y\right) \qquad \text{If } |y| > 1$$

(33a-e)

Where $\left[x\right]$ is the "nearest integer" function, or $nint\left(x\right)$, also known as the "Round" function, $Round\left[x\right]$, which takes a real number and returns the closest integer to the original real number; if x is equally close to both integers then the function returns the even-numbered integer. Note that $K_{\max}$ is a prescribed arbitrary maximum mode number. Further, it should be assumed that $K_{\max}$ is even and therefore symmetric. The above analysis, with and without azimuthal corrections, provides a first-order insight into the spatiotemporal distribution of vortex disturbance velocities subjected to modal excitation. When k is even the mode and disturbance velocity distributions are symmetric; when k is odd then the mode and disturbance velocities are asymmetric. This approximate disturbance velocity analysis is applicable to a wide range of (laminar) basic flow solutions for vortical flow.

Finally, one means of assessing the relative flow "stability" of the vortex filament as a function of time and initial conditions can be provided by the parameter, ϑ, defined below.

$$\vartheta \equiv \vartheta_1 / \vartheta_0$$

$$\vartheta_1 \equiv \int_{-L/2}^{L/2} \int_{0^+}^{\infty^-} \tilde{\xi} r dr dz$$

$$\vartheta_0 \equiv \left. \int_{-L/2}^{L/2} \int_{0^+}^{\infty^-} \xi r dr dz \right|_{t=0^+}$$

$$\tilde{\xi} \equiv \frac{1}{\pi} \int_0^{\pi/\omega_n} \hat{\xi} dt^\bullet$$

$$\hat{\xi} \equiv \hat{v}_\theta^2 + \hat{v}_r^2 + \hat{v}_z^2 \qquad \left| z^\bullet \right| > z_w^\bullet$$

$$\hat{\xi} \equiv 0 \qquad \left| z^\bullet \right| \le z_w^\bullet$$

(34a-b)

Note the analogous nature of the aggregate (instability) disturbance parameter, ϑ, defined in Eq. 34a-b, with respect to the effectiveness and efficiency parameters, η_V and β_V noted earlier in the main body of the paper. The current suggested form of the global (instability) disturbance parameter, ϑ, takes into account only two discrete arbitrary modes at a time -- the nth and mth modes -- rather than some prescribed distribution of modes.

An approximate relationship for the disturbance parameter, used in the main body of the paper, is given by the expression

$$\frac{\tilde{\xi}^\bullet}{a_1^2} \approx e^{2\left(\int (1/A) dz^\bullet - r^\bullet\right)} \left\{ \left(\frac{1}{A^2} \left(\frac{\partial A}{\partial z^\bullet} - 1 \right) - \int \left(\frac{1}{A^2} \frac{\partial A}{\partial r^\bullet} \right) dz^\bullet + 1 \right)^2 + \frac{1}{A^2} + 1 \right\} \tag{35}$$

Given the above expression, the disturbance parameter, ϑ, can be normalized (approximately so) by the excitation amplitude, a_1, for one or two dominant excitation modes such that $\vartheta / a_1^2 \approx constant$ for a given small range of $t^\bullet$.

An interesting question to consider is whether or not Eqs. 27a-b and 28 genuinely represent unstable versus stable or neutral flow. As there is no unconstrained amplification of the a parameter (or, rather, the a_n, nth mode, amplitude) excitation with time, this would suggest that the flow, for $b \approx 1$, is stable or neutral. If, on the other hand, $b << 1$ for some finite period of time then the approximate solution would suggest the possibility, at least, of unconstrained disturbance velocities at the outer radial regions of the vortex filament.